Characterization of atomic state evolution in the JC and anti-JC models: spin-displaced field modes in the quantum Rabi model

Preprint · March 2023

DOI: 10.13140/RG.2.2.23959.75682

1 author:

Joseph Akeyo Omolo
Maseno University
39 PUBLICATIONS **77** CITATIONS

SEE PROFILE

Characterization of atomic state evolution in the JC and anti-JC models: spin-displaced field modes in the quantum Rabi model

Joseph Akeyo Omolo
Department of Physics, Maseno University, P.O. Private Bag, Maseno, Kenya
e-mail: ojakeyo@maseno.ac.ke / ojakeyo04@yahoo.co.uk

20 March 2023

Abstract

In this article, characterization of the atomic state evolution in the Jaynes-Cummings (JC) and anti-Jaynes-Cummings (aJC) models means using the reduced atomic state degree of purity, concurrence and spin excitation number to determine the ranges and critical values of the mean photon number and frequency detuning parameters at which the atom is in a disentangled pure, mixed or entangled state. By unifying the mean photon number amplitude and detuning parameters in a simple relation, leaving the mean photon number as the only variable parameter, we have discovered a beautiful natural evolution property where the atom is in a uniformly mixed state describing symmetrical stable evolution of collapses and revivals of the degree of purity and concurrence, one above and the other below, a uniformly mixed state axis through points of equal degree of purity and concurrence at $\frac{1}{\sqrt{2}}$, with the revival turning points coinciding on the axis. Within the small mean photon number $\overline{n}$ range $0 < \sqrt{\overline{n}} \leq 0.1$, evolution from an initial ground state $|g0\rangle$ remains in a pure plane wave ground state in resonant strong coupling JC model, but develops into an entangled state describing pure Rabi oscillations between the qubit states $|g0\rangle$ and $|e1\rangle$ in the resonant strong coupling aJC model. The resonance strong coupling evolution is in a mixed state in the range $0.1 < \sqrt{\overline{n}} < 1$, developing collapses and revivals, with spontaneous evolution to short-lived, very nearly disentangled pure state, within the range $1 < \sqrt{\overline{n}} \leq 8.55$ in both models. In resonant weak coupling aJC model, increasing a residual detuning parameter to very large values generates steady state time-independent evolution of the state measures at their appropriate maximum or minimum values, signifying the atom in a completely disentangled pure state, stable mixed state or stable entangled state, within well defined ranges of the mean photon number, up to a maximum $\sqrt{\overline{n}}_{max} = 11.2$, where the evolution reaches and remains in a maximally entangled state completely independent of detuning. Similar ground state, mixed state, entangled state and maximally entangled state evolution regimes, developing into steady state time-independent evolution, are also achievable in the off-resonance JC and aJC models. In general, the atomic state evolves asymptotically to a maximally entangled state over long interaction times. Finally, at a triple resonance property where the atomic state transition frequency, field mode frequency and the atom-field mode coupling constant are all equal, the quantum Rabi model reduces to JC and aJC spin-displaced field modes with well defined spectrum of energy eigenstates and eigenvalues.

1 Introduction

The current state of development of quantum information processing and related quantum technologies needs a much better understanding of models of interacting fully quantized systems. The best model is achieved by specifying well defined qubit states and transition operators which constitute the basic structure of the dynamical evolution of the system. In general, an interaction drives a system from an initial qubit state into a superposition of qubit states, signifying the development of state coherence or entanglement properties used as resources in quantum information processing, providing a general framework for quantum computation, teleportation, communication, metrology, etc.

For example, the interaction of a quantized electromagnetic field initially in the vacuum state $|0\rangle$ with a classical electric current drives the field into a superposition of the number states $|n\rangle$, while the interaction of a two-level atom initially in the ground (excited) state $|g\rangle$ ($|e\rangle$) with a classical electromagnetic field drives the atom into a superposition of the ground and excited states. The superposition of the number states

constitutes a coherent state of the quantized light, while the superposition of atomic spin states constitutes a coherent state of the atom. These are interesting alternate examples of semiclassical light-matter interactions in which classical matter drives quantized light to a coherent state, while in the alternative model, classical light drives quantized matter (two-level atom) to a coherent state. The question which immediately arises is, what is the characteristic property of superposition states in a fully quantized light-matter interaction ?. The answer is already well known in general form, which we address in greater detail in the present article.

A simple generalization to a fully quantized light-matter interaction consists of a two-level atom interacting with a quantized electromagnetic field mode, known as the quantum Rabi model. Decomposition of the quantum Rabi model into the algebraically inseparable Jaynes-Cummings (JC) and anti-Jaynes-Cummings (aJC) components, each with a conserved excitation number operator, provides an exactly solvable qubit interpretation [1 , 2] where the fully quantized light-atom interactions in the JC and aJC components treated separately develop into superpositions of the respective qubit states, thus generally forming an entangled light-atom state. The general time evolving entangled state describes dynamical evolution with collapses and rivals of Rabi oscillations of excitations in the coupled qubit states.

In the current qubit interpretation of the quantum Rabi model defined explicitly below, it has been established that the JC and aJC interaction models are duality symmetry conjugates, transforming into each other through a duality symmetry operation [3]. The duality symmetry conjugation property means that the JC and aJC models may be treated separately without the need for an approximation, such as the rotating wave approximation (RWA) which has been applied over the years from 1963 [4] to reduce the quantum Rabi model to the single exactly solvable JC component.

In the physics framework, the JC interaction mechanism generates *red-sideband* atom-field mode qubit state transitions characterized by difference frequency detuning $\delta = \omega_0 - \omega$, while the aJC interaction mechanism generates *blue-sideband* atom-field mode qubit state transitions characterized by sum frequency detuning $\overline{\delta} = \omega_0 + \omega = \delta + 2\omega$, meaning that the aJC model has a non-vanishing residual detuning 2ω even under resonance $\omega_0 = \omega$ when the JC detuning vanishes ($\delta = 0$). The existence of the non-vanishing residual detuning of the aJC component then means that the full quantum Rabi model also has a non-vanishing residual detuning 2ω, which may generally have been ignored, yet contributing significantly to the observed dynamics in theoretical and experimental studies. A very important, essentially fundamental, physical property is that the aJC interaction mechanism has non-zero excitations in the ground state $|g0\rangle$ and generates blue-sideband transitions from the ground state, characterized by a time evolving entangled state describing Rabi oscillations between the qubit states $|g0\rangle$ and $|e1\rangle$, while, on the other hand, the ground state $|g0\rangle$ is an eigenstate of the JC Hamiltonian, which therefore does not cause transitions, but generates only a pure plane wave time evolution of the ground state. The important physical property that the aJC component has non-zero excitations and generates qubit transitions from the ground state $|g0\rangle$ obviously shows up, and may be responsible for some observed effects, in the full quantum Rabi dynamics from an initial ground state $|g0\rangle$ generally preferred in experiments [5].

The clear understanding of the JC-aJC duality symmetry conjugation property and the internal physical property that the aJC interaction mechanism has a non-vanishing residual detuning and naturally generates blue-sideband transitions from the ground state, strongly motivate a revisiting of the dynamics of the quantum Rabi model, which have treated (partly) in this article through characterization of the atomic state evolution, separately in both JC and aJC models. Characterization of the atomic state in the JC and aJC models as developed here means specifying the ranges of values, and determining the critical values, of physical parameters such as the mean photon number and frequency detunings where the atomic state, described by a reduced density operator from the light-atom superposition state, is pure, mixed or entangled, and if a coherent state property arises as in the corresponding semiclassical light-atom interactions. This is particularly important for atomic state preparations, noting that in earlier studies of the atomic state evolution in the JC model [6-11], it has been assumed that a disentangled pure state emerges in the limit of very large mean photon number $\overline{n} \to \infty$, whereas the evolution obtained in the present study reveals that the atom-field mode state is maximally entangled, not pure, at $\sqrt{\overline{n}} \geq 11.2$, meaning that the original derivations in [6 , 7 , 8 , 11] need a reinterpretation of the $\overline{n} \to \infty$ approximation.

The earlier studies in resonant JC model, separately using the reduced atomic state purity measure [6] , von Newman entropy [9] and nonclassicality quantifier [12], revealed spontaneous evolution to a *short-lived*, very nearly, pure state in the middle of the first collapse period of the atomic state population inversion. In the present article, we have used the reduced atomic state degree of purity, concurrence and spin excitation number in both resonant JC and aJC models to establish that the spontaneous evolution to a short-lived very nearly pure state in the middle of the collapse period of the spin excitation number (or the related

state population inversion) generally occurs within the mean photon number range $1 < \sqrt{\overline{n}} \leq 8.55$, allowing a maximum mean photon number $\overline{n}_{max} = (8.55)^2$. The approximate form of the disentangled pure state derived in [6 , 7] and the related studies, must thus be limited to large mean photon number $\overline{n} \leq (8.55)^2$. For larger values $8.55 < \sqrt{\overline{n}} < 11.2$, the atomic state evolution is effectively in the mixed and entangled state regimes, finally reaching and remaining in, the maximally entangled state at $\sqrt{\overline{n}} \geq 11.2$.

In this article, we use the reduced atomic state degree of purity, concurrence and spin excitation number derived in an earlier article [13] to provide a comprehensive characterization of the atomic state evolution in resonance and off-resonance JC and aJC dynamics. In unifying the mean photon number amplitude $\sqrt{\overline{n}}$ and the frequency detuning parameters, leaving the mean photon number amplitude as the only variable physical parameter, we have discovered a beautiful dynamical phenomenon, which we identify as *natural evolution* in a *uniformly mixed state*. In natural evolution, the collapses and revivals of the degree of purity and concurrence evolve symmetrically, one above and the other below, an axis passing through points where the degree of purity and concurrence are equal, at $\frac{1}{\sqrt{2}}$, identified as the *uniformly mixed state*-axis. The revival turning points of the degree of purity and concurrence coincide on the uniformly mixed state axis. The regular symmetrical, nearly periodic, pattern of evolution about the uniformly mixed state axis leads to an interpretation of the natural evolution property as a simple generalization of the resonance property to include off-resonance dynamics, fixed by a relation unifying the mean photon number and the detuning parameters. Keeping the mean photon number amplitude fixed at the natural evolution value, but progressively increasing the detuning parameter generates periodic evolution in mixed states in the intermediate stages, developing into *steady state* time-independent evolution signifying exact completely disentangled pure states or stable mixed states or stable entangled states, noting that a maximally entangled state reached at $\sqrt{\overline{n}} \geq 11.2$ is completely independent of the detuning parameters. We have also discovered an interesting physical property that, under *triple resonance* condition where the field mode frequency ω, the atomic state transition frequency ω_0 and the atom-field mode coupling constant λ are all equal as $\lambda = \omega = \omega_0$, the JC qubit reduces to a JC spin-displaced field mode, with the aJC spin-displaced field mode arising as the duality symmetry conjugate.

We begin with a brief description of the quantum Rabi model in the JC and aJC qubit interpretation in section 2, where we provide a complete general solution of the reduced density operator of the atom and evaluate the degree of purity, concurrence and spin excitation number in each model. In section 3, we present the characterization of the atomic state evolution, subdivided into natural evolution property in 3.1, resonance dynamics in 3.2, off-resonance dynamics in 3.3. We introduce the triple resonance property of intermediate coupling interaction and develop the resulting spin-displaced field modes in section 3.4. We close with the Conclusion in section 4.

2 Atomic state in the JC and aJC models

The basic model of a two-level atom interacting with a single quantized mode of electromagnetic field is the quantum Rabi model defined by Hamiltonian

$$H_R = \hbar\omega \left(\hat{a}^\dagger \hat{a} + \frac{1}{2}\right) + \frac{1}{2}\hbar\omega_0\sigma_z + \hbar g(\hat{a}^\dagger + \hat{a})\sigma_x \tag{1}$$

where $\sigma_z, \sigma_\pm, \sigma_x = \sigma_+ + \sigma_-$, ω_0 and $\hat{a}, \hat{a}^\dagger, \omega$ are the respective atomic spin and field mode state transition operators and angular frequencies in standard definition. Here, we have included the field mode ground state energy $\frac{1}{2}\hbar\omega$ for anticipated symmetrization of the Hamiltonian H_R as a sum of JC and aJC Hamiltonians. Since the Pauli spin operators are used as order parameters for studying the dynamical properties of the atom, we define them explicitly in terms of the atomic ground state $|g\rangle$ and excited state $|e\rangle$ in standard form

$$\sigma_+ = |e\rangle\langle g| \; ; \qquad \sigma_- = |g\rangle\langle e| \; ; \qquad I = \sigma_+\sigma_- + \sigma_-\sigma_+ \; ; \qquad \sigma_z = \sigma_+\sigma_- - \sigma_-\sigma_+$$
$$\sigma_x = \sigma_+ + \sigma_- \; ; \qquad \sigma_y = -i(\sigma_+ - \sigma_-) \tag{2}$$

The JC and aJC models are the rotating and antirotating components of the quantum Rabi model. From the very beginning, the JC model has been known to have a conserved excitation number operator, which allows exact solutions through a diagonalization method yielding eigenstates and eigenvalues of the Hamiltonian [4]. This encouraged and enabled intensive theoretical and experimental studies of the general dynamical and fundamental quantum mechanical features of the atom-field interaction within the weak-coupling regime where the JC model is effective. On the other hand, the aJC component was believed to violate the energy

conservation principle and therefore its dynamical properties were never studied directly, until the year 2017 when the present author applied basic algebraic properties to construct and prove conservation of an excitation number operator for the aJC model [1]. The existence of conserved excitation number operators has led to a simple physically intuitive and exactly solvable polariton and antipolariton qubit interpretation [14], where the JC (polariton) qubit is characterized by a conserved excitation number operator $\hat{N}$ and red-sideband state transition operator $\hat{R}$, while the aJC (antipolariton) qubit is characterized by a conserved excitation number operator $\hat{\overline{N}}$ and blue-sideband state transition operator $\hat{\overline{R}}$, presented in comprehensive form in [2]. In the qubit interpretation, a dynamical picture emerges that the JC and aJC models are two algebraically inseparable components of the quantum Rabi model with Hamiltonian H_R reformulated in symmetrized JC (polariton) and aJC (antipolariton) qubit form [1 , 2 , 3 , 14]

$$H_R = \frac{1}{2}(H_{JC} + H_{aJC})$$

$$H_{JC} = \hbar\omega\hat{N} + \hbar\hat{R} \quad ; \quad \hat{N} = \hat{a}^\dagger\hat{a} + \frac{1}{2}\sigma_z = \hat{a}^\dagger\hat{a} + \sigma_+\sigma_- - \frac{1}{2} \quad ; \quad \hat{R} = \frac{1}{2}(\omega_0 - \omega)\sigma_z + \lambda(\hat{a}\sigma_+ + \hat{a}^\dagger\sigma_-)$$

$$H_{aJC} = \hbar\omega\ \hat{\overline{N}} + \hbar\hat{\overline{R}} \quad ; \quad \hat{\overline{N}} = \hat{a}\hat{a}^\dagger - \frac{1}{2}\sigma_z = \hat{a}\hat{a}^\dagger + \sigma_-\sigma_+ - \frac{1}{2} \quad ; \quad \hat{\overline{R}} = \frac{1}{2}(\omega_0 + \omega)\sigma_z + \lambda(\hat{a}\sigma_- + \hat{a}^\dagger\sigma_+)$$

$$\lambda = 2g \tag{3}$$

where $(\hat{N}\ ,\ \hat{R})$, $(\ \hat{\overline{N}}\ ,\ \hat{\overline{R}}\ )$ are the respective conserved excitation number and qubit state transition operators, while $(\omega_0 - \omega)$, $(\omega_0 + \omega)$ are the JC red-sideband and aJC blue-sideband atom-field frequency detunings. Note that, due to the symmetrization, the coupling constant λ in the JC , aJC Hamiltonians H_{JC} , H_{aJC} is double the coupling constant g in the quantum Rabi Hamiltonian H_R in equation (1), i.e., $\lambda = 2g$ as defined in equation (3). In [3], it has been established that the JC qubit Hamiltonian H_{JC} and the aJC qubit Hamiltonian H_{aJC} are duality symmetry conjugates transforming into each other through a duality symmetry operation.

The important characteristic features of the aJC interaction mechanism compared to the JC interaction mechanism, which we explained earlier, are now evident in equation (3): (i) at resonance $\omega = \omega_0$ where the JC detuning $\omega_0 - \omega$ vanishes, the aJC detuning $\omega_0 + \omega$ always has a non-vanishing residual detuning equal to twice the field mode frequency (2ω), meaning that the aJC dynamics is generally detuned, revealing the important property that the quantum Rabi model as defined in equation (3) is internally detuned (ii) with the atom in the ground state $|g\rangle$ and the field mode in the vacuum state $|0\rangle$, the aJC interaction mechanism generates blue-sideband transitions $|g0\rangle \rightarrow |e1\rangle$ with dynamical evolution characterized by Rabi oscillations between the qubit states, which cannot be achieved in the JC interaction mechanism, since the ground state $|g0\rangle$ is an eigenstate of the JC Hamiltonian H_{JC}, as in equations (22) , (23) , (24) below (iii) an important feature not immediately evident in equation (3) is that the aJC interaction mechanism generates purely sub-Poissonian photon statistics, compared with the generally super-Poissonian photon statistics in the JC model [15]. These interesting dynamical features of the aJC model are important for practical applications in quantum information processing and related quantum technologies, yet they have not received much, if any, attention in the existing published literature. It is therefore necessary to present an in-depth theoretical study of the general dynamics of the aJC model to provide a useful framework for experiments and practical applications.

As we explained earlier, the property that the JC and aJC models are duality symmetry conjugates allows us to treat them separately. In a strict sense, the duality symmetry property means that we determine only the general time evolving state vector of one component, JC or aJC, explicitly and then obtain the state vector of the other component through the duality symmetry conjugation operation. However, to remain consistent with the specification of an initial state of the atom-field interaction in the full quantum Rabi model, we consider both JC and aJC interactions from the same initial state and determine the respective general time evolving state vectors separately. Since a comprehensive characterization of the atomic state evolution using the degree of purity, concurrence and spin excitation number has not been done in the JC model as well, we treat both models side by side in this article.

For direct comparison of results with earlier original studies in the JC model [6 , 9 , 11 , 12], we consider the atom-field initial state $|\psi_{g\alpha}\rangle$, where the atom is in the ground state $|g\rangle$ and the field mode is in a coherent state $|\alpha\rangle$, expressed as a superposition of the field mode number (Fock) states $|n\rangle$. The atom-field mode initial

state in the JC and aJC models then takes the product form

$$|\psi_{g\alpha}\rangle = \sum_{n=0}^{\infty} \frac{e^{-\frac{1}{2}\alpha^2}\alpha^n}{\sqrt{n!}}|gn\rangle \tag{4}$$

A systematic method for determining the general time evolving state vector generated by the time evolution operators $U_{JC}(t) = e^{-\frac{i}{\hbar}H_{JC}t}$, $U_{aJC}(t) = e^{-\frac{i}{\hbar}H_{aJC}t}$ from the initial state in equation (4) is presented in detail in [13], where the original formulation of the atomic state dynamics in the JC and aJC models in the present context was developed. We present only the final results here.

In the JC model with qubit Hamiltonian H_{JC} in equation (3), the general time evolving state vector $|\Psi_{JC}(t)\rangle$ is obtained and reorganized (Schmidt decomposition) in the form,

$$|\Psi_{JC}(t)\rangle = \sum_{n=0}^{\infty}(\sqrt{P_n}e^{-i\omega nt}(\cos(R_n t) + ic_n \sin(R_n t))|g\rangle - i\sqrt{P_{n+1}}e^{-i\omega(n+1)t}s_{n+1}\sin(R_{n+1}t)|e\rangle)|n\rangle$$

$$R_n = \lambda\sqrt{n + \frac{1}{4}\beta^2}\ ; \quad c_n = \frac{\omega_0 - \omega}{2R_n}\ ; \quad R_{n+1} = \lambda\sqrt{n+1+\frac{1}{4}\beta^2}\ ; \quad s_{n+1} = \frac{\lambda\sqrt{n+1}}{R_{n+1}}\ ; \quad \beta = \frac{\omega_0-\omega}{\lambda} \tag{5}$$

while in the aJC model with qubit Hamiltonian H_{aJC} in equation (3), the general time evolving state vector $|\Psi_{aJC}(t)\rangle$ is obtained and reorganized in the form

$$|\Psi_{aJC}(t)\rangle = \sum_{n=0}^{\infty}(\sqrt{P_n}e^{-i\omega(n+1)t}(\cos(\overline{R}_{n+1}t) + i\overline{c}_{n+1}\sin(\overline{R}_{n+1}t))|g\rangle - i\sqrt{P_{n-1}}e^{-i\omega nt}\overline{s}_n\sin(\overline{R}_n t)|e\rangle)|n\rangle$$

$$\overline{R}_{n+1} = \lambda\sqrt{n+1+\frac{1}{4}\overline{\beta}^2}\ ; \quad \overline{c}_{n+1} = \frac{\omega_0+\omega}{2\overline{R}_{n+1}}\ ; \quad \overline{R}_n = \lambda\sqrt{n+\frac{1}{4}\overline{\beta}^2}\ ; \quad \overline{s}_n = \frac{\lambda\sqrt{n}}{\overline{R}_n}\ ; \quad \overline{\beta} = \frac{\omega_0+\omega}{\lambda} \tag{6}$$

where in each case in equations (5) , (6), the photon distribution probabilities are defined by

$$P_{n+j} = \frac{e^{-\overline{n}}\,\overline{n}^{(n+j)}}{(n+j)!}\ ; \quad \alpha = \sqrt{\overline{n}}\ ; \quad j = 0, 1, -1 \tag{7}$$

where we have introduced the mean photon number $\overline{n}$ to define the real amplitude $\alpha = \sqrt{\overline{n}}$. Since we have used the full qubit Hamiltonians H_{JC} , H_{aJC}, the general solutions in equations (5) , (6) include the time evolving global phase factors $e^{-i\omega nt}$, $e^{-i\omega(n+1)t}$ generated by the excitation number operator components $\hbar\omega\hat{N}$, $\hbar\omega\hat{\overline{N}}$. Note that we have dropped a common factor $e^{-\frac{i}{2}\omega t}$.

In the definitions of the Rabi oscillation frequencies R_{n+j} , $\overline{R}_{n+j}$, $j = 0, 1$ in equations (5) , (6), we have introduced dimensionless JC and aJC detuning parameters β , $\overline{\beta}$ as defined above. Noting that these are defined in terms of ω_0 , ω, we reduce the parameter choices by considering that, in general, the frequency detuning $\omega_0 \mp \omega$, means that the atomic state transition angular frequency ω_0 is related to the field mode angular frequency ω by a numerical factor k in the form $\omega_0 = k\omega$, where the value $k = 1$ specifies the resonance condition. Using this relation in equations (5) , (6) and introducing a dimensionless parameter f defined by $\omega = f\lambda$, the dimensionless JC and aJC detuning parameters β , $\overline{\beta}$ now take the simple form

$$\omega_0 = k\omega\ ; \qquad \Rightarrow \qquad \beta = (k-1)f\ ; \qquad \overline{\beta} = (k+1)f\ ; \qquad f = \frac{\omega}{\lambda}\ ; \qquad k > 0 \tag{8}$$

which, for given $k > 0$ (automatically fixed by the values of ω_0 , ω), depends only on the dimensionless parameter f. We identify k as the dimensionless atom-field mode frequency detuning parameter. Resonance dynamics is specified by $k = 1$. It follows that, under resonance $k = 1$, the JC and aJC detuning parameters β , $\overline{\beta}$ in equation (8) take the form

$$\textbf{Resonance}\ ; \quad k = 1\ : \quad \text{JC}\ : \quad \beta = 0\ ; \qquad \text{aJC}\ : \quad \overline{\beta} = 2f \tag{9}$$

which shows that, in resonance dynamics specified by $k = 1$ and generally defined by $\omega = \omega_0$, the JC detuning vanishes ($\beta = 0$), while the aJC detuning reduces to $\overline{\beta} = 2f$. Since the field mode frequency never vanishes ($\omega > 0$), the dimensionless parameter $f = \frac{\omega}{g}$ also never vanishes ($f > 0$). Noting that f defines the detuning parameters according to equations (8) , (9), we have identified $f > 0$ as the non-vanishing *residual* detuning

parameter. The important physical property which we reemphasize here is that the JC detuning vanishes at resonance, while the aJC interaction remains detuned both in-resonance ($k = 1\ ,\ \omega = \omega_0$) and off-resonance ($k \neq 1\ ,\ \omega \neq \omega_0$), meaning that the quantum Rabi model defined by $H_R = \frac{1}{2}(H_{JC} + H_{aJC})$ in equation (3) is *intrinsically detuned*, thus experiencing effects of detuning both in-resonance and off-resonance.

Substituting $\beta = (k-1)f\ ,\ \overline{\beta} = (k+1)f$ from equation (8) into equations (5) , (6), the Rabi frequencies $R_{n+j}\ ,\ \overline{R}_{n+j},\ j = 0, 1$ and the related interaction parameters take the form

$$\text{JC}\ :\quad R_{n+j} = \lambda\sqrt{n+j+\frac{1}{4}(k-1)^2 f^2}\ ;\qquad c_{n+j} = \frac{(k-1)f}{2\sqrt{n+j+\frac{1}{4}(k-1)^2 f^2}}$$

$$s_{n+j} = \frac{\sqrt{n+j}}{\sqrt{n+j+\frac{1}{4}(k-1)^2 f^2}}$$

$$\text{aJC}\ :\quad \overline{R}_{n+j} = \lambda\sqrt{n+j+\frac{1}{4}(k+1)^2 f^2}\ ;\qquad \overline{c}_{n+j} = \frac{(k+1)f}{2\sqrt{n+j+\frac{1}{4}(k+1)^2 f^2}}$$

$$\overline{s}_{n+j} = \frac{\sqrt{n+j}}{\sqrt{n+j+\frac{1}{4}(k+1)^2 f^2}}\ ;\quad j = 0, 1 \tag{10}$$

Substituting the photon distribution probabilities P_{n+j}, field mode frequency $\omega = f\lambda$, Rabi frequencies $R_{n+j}\ ,\ \overline{R}_{n+j}$ and the related parameters from equations (7) , (8) , (10) into the general time evolving state vectors in equations (5) , (6) and introducing scaled time $\tau = \lambda t$ then means that the only parameters which characterize the dynamical evolution in the JC and aJC models are the mean photon number amplitude $\sqrt{\overline{n}}$ of the coherent field mode and the non-vanishing residual detuning parameter f, noting that the numerical factor k is automatically fixed by the atomic state transition and field mode frequencies $\omega_0\ ,\ \omega$ according to the relation in equation (8).

We observe that, by its definition as the ratio of the field mode angular frequency ω to the atom-field mode coupling constant g in equation (8), the dimensionless residual detuning parameter $f = \frac{\omega}{\lambda}$ specifies the coupling regimes in both JC and aJC models, noting that f is essentially the inverse of the coupling strength in standard definitions used in [5] and related works. The strong coupling interaction characterized by $g > \omega$ is specified by parameter values $0 < f < 1$, the weak coupling interaction characterized by $g < \omega$ is specified by $f > 1$ and the intermediate coupling interaction characterized by $g = \omega$ is specified by $f = 1$. Hence, specifying the residual detuning parameter values within the range $0 < f < 1$ characterizes strong coupling interaction, while values in the open range $f > 1$ ($1 < f < \infty$) characterizes weak coupling interaction and the specific boundary value $f = 1$ characterizes an interesting intermediate coupling interaction where the JC and aJC qubit Hamiltonians each factorizes precisely as a normal order product of spin-displaced bipartite state annihilation and creation operators, forming the Hamiltonian of a spin-displaced field mode with an exact spectrum of energy eigenstates. The aJC spin-displaced field mode is directly interpreted as a duality-symmetry conjugate of the JC spin-displaced field mode. Interestingly, the factorization into a spin-displaced field mode operators may be related to the interaction mechanism at the quantum phase transition of the JC model at critical coupling $\lambda_c = 2g_c = \sqrt{\omega_0\omega}$, equivalent to the established critical coupling of the full quantum Rabi model at $g_c = \frac{1}{2}\sqrt{\omega_0\omega}$.

The general dynamics of the bipartite atom-field system is described by a density operator $\rho_{JC}(t) = |\Psi_{JC}(t)\rangle\langle\Psi_{JC}(t)|$ in the JC model and $\rho_{aJC}(t) = |\Psi_{aJC}(t)\rangle\langle\Psi_{aJC}(t)|$ in the aJC model. The general dynamics of the atom is described by the respective reduced density operators $\rho_a(t)\ ,\ \overline{\rho}_a(t)$ obtained by tracing out the field mode states from the corresponding bipartite density operators according to

$$\rho_a(t) = Tr_f\rho_{JC}(t) = Tr_f|\Psi_{JC}(t)\rangle\langle\Psi_{JC}(t)|\ ;\qquad \overline{\rho}_a(t) = Tr_f\rho_{aJC}(t) = Tr_f|\Psi_{aJC}(t)\rangle\langle\Psi_{aJC}(t)| \tag{11}$$

Substituting the JC and aJC general time evolving state vectors $|\Psi_{JC}(t)\rangle\ ,\ |\Psi_{aJC}(t)\rangle$ from equations (5) , (6) , (7) into equation (11) as appropriate provides the atomic state reduced density operator $\rho_a(t)$ in the JC model in the explicit form (details in [13])

$$\text{JC}:\qquad \rho_a(t) = \frac{1}{2}(1 + \mathbf{r}\cdot\vec{\sigma})\ ;\qquad \mathbf{r} = (r_1\ ,\ r_2\ ,\ r_3)$$

$$r_3 = \sum_{n=0}^{\infty} P_{n+1} s_{n+1}^2 \sin^2(R_{n+1}t) - \sum_{n=0}^{\infty} P_n(\cos^2(R_n t) + c_n^2 \sin^2(R_n t))$$

$$r_1 = -2\sum_{n=0}^{\infty} \sqrt{P_{n+1}P_n}\, s_{n+1} \sin(R_{n+1}t)(\sin(\omega t)\cos(R_n t) + c_n \cos(\omega t)\sin(R_n t)\ )$$

$$r_2 = 2\sum_{n=0}^{\infty} \sqrt{P_{n+1}P_n}\, s_{n+1} \sin(R_{n+1}t)(\cos(\omega t)\cos(R_n t) - c_n \sin(\omega t)\sin(R_n t)\ )$$

$$\mathrm{Tr}\rho_a(t) = 1 \tag{12}$$

and the atomic state reduced density operator $\overline{\rho}_a(t)$ in the aJC model in the explicit form

$$\text{aJC}: \qquad \overline{\rho}_a(t) = \frac{1}{2}(1 + \overline{\mathbf{r}} \cdot \vec{\sigma})\ ; \qquad \overline{\mathbf{r}} = (\overline{r}_1\ ,\ \overline{r}_2\ ,\ \overline{r}_3)$$

$$\overline{r}_3 = \sum_{n=0}^{\infty} P_{n-1} \overline{s}_n^2 \sin^2(\ \overline{R}_n t) - \sum_{n=0}^{\infty} P_n(\cos^2(\ \overline{R}_{n+1}t) + \overline{c}_{n+1}^2 \sin^2(\ \overline{R}_{n+1}t))$$

$$\overline{r}_1 = 2\sum_{n=0}^{\infty} \sqrt{P_n P_{n-1}}\, \overline{s}_n \sin(\ \overline{R}_n t)(\sin(\omega t)\cos(\ \overline{R}_{n+1}t) - \overline{c}_{n+1}\cos(\omega t)\sin(\ \overline{R}_{n+1}t)\ )$$

$$\overline{r}_2 = 2\sum_{n=0}^{\infty} \sqrt{P_n P_{n-1}}\, \overline{s}_n \sin(\ \overline{R}_n t)(\cos(\omega t)\cos(\ \overline{R}_{n+1}t) + \overline{c}_{n+1}\sin(\omega t)\sin(\ \overline{R}_{n+1}t)\ )$$

$$\mathrm{Tr}\overline{\rho}_a(t) = 1 \tag{13}$$

In equations (12) , (13), $\mathbf{r} = (r_1\ ,\ r_2\ ,\ r_3)$, $\overline{\mathbf{r}} = (\overline{r}_1\ ,\ \overline{r}_2\ ,\ \overline{r}_3)$, are the respective radius vectors of the Bloch spheres of the atomic states in the JC and aJC models, while $\vec{\sigma} = (\sigma_x\ ,\ \sigma_y\ ,\ \sigma_z) \equiv (\sigma_1\ ,\ \sigma_2\ ,\ \sigma_3)$ is the Pauli spin operator vector defined in equation (2). The important feature which emerges here is that the coherence components $(r_1\ ,\ r_2)$, $(\overline{r}_1\ ,\ \overline{r}_2)$ in equations (12) , (13), are modulated by the periodically time varying field mode frequency-dependent factors $\sin(\omega t)$, $\cos(\omega t)$ from the respective free evolution global phase factors $e^{-i\omega n t}$, $e^{-i\omega(n+1)t}$ of the general solutions in equations (5) , (6). In general, the Bloch sphere radius vector components r_j , $\overline{r}_j$ are obtained as the mean values of the corresponding Pauli spin operators σ_j with respect to the respective reduced density operators $\rho_a(t)$, $\overline{\rho}_a(t)$ of the atom in the respective JC , aJC model according to

$$r_j = Tr\sigma_j\rho_a(t)\ ; \qquad \overline{r}_j = Tr\sigma_j\overline{\rho}_a(t)\ ; \quad j = 1,2,3 \equiv x,y,z \tag{14}$$

The determination of the reduced density operators $\rho_a(t)$, $\overline{\rho}_a(t)$ in explicit form in equations (12) , (13) constitutes a complete general solution for describing the dynamics of the atom in the JC and aJC models. According to the general definitions in equation (14), the Bloch vector components r_3 , $\overline{r}_3$ describe the atomic state population inversion, related to the respective atomic spin excitation numbers in the form

$$\text{JC}\ :\quad \langle\sigma_+\sigma_-\rangle = Tr\sigma_+\sigma_-\rho_a(t) = \frac{1}{2}(1 + r_3)\ ; \qquad \text{aJC}\ :\quad \langle\sigma_-\sigma_+\rangle = Tr\sigma_-\sigma_+\overline{\rho}_a(t) = \frac{1}{2}(1 - \overline{r}_3) \tag{15}$$

while the components $(r_1\ ,\ r_2)$, $(\overline{r}_1\ ,\ \overline{r}_2)$ describe the coherence properties of the atom.

The Bloch sphere is the geometrical configuration containing possible quantum states of the atom. The states are distributed inside and on the surface of the sphere, where the states inside are mixed states, while the states on the surface are pure states. The time evolution of the Bloch radius $r = \sqrt{r_1^2 + r_2^2 + r_3^2}$, $\overline{r} = \sqrt{\overline{r}_1^2 + \overline{r}_2^2 + \overline{r}_3^2}$ describes the evolution of the quantum states of the atom.

A complete description of the atomic state evolution is provided by the state purity operator $\rho_a^2(t)$ in the JC model and $\overline{\rho}_a^2(t)$ in the aJC model. As developed in great detail in [13], all the characteristic elements of measures of atomic state purity or entanglement are derivable from the state purity operator. From these derivations, we have introduced a degree of purity and concurrence, which are complementary measures of state purity or entanglement, intricately connected by a complementarity relation.

With the normalized reduced density operators $\rho_a(t)$, $\overline{\rho}_a(t)$ in equations (12) , (13), the atomic state purity operators in the JC and aJC models are obtained in the explicit form (details in [13])

$$\text{JC}\ :\quad \rho_a^2 = \rho_a - \mathcal{M}I\ ; \quad \mathcal{M} = \frac{1}{4}(1 - r^2)\ = \det\rho_a\ ; \quad r = |\mathbf{r}|\ = \sqrt{r_1^2 + r_2^2 + r_3^2}$$

$$\text{aJC} \;:\quad \overline{\rho}_a^2 = \overline{\rho}_a - \overline{\mathcal{M}} I \;;\quad \overline{\mathcal{M}} = \frac{1}{4}(1-\overline{r}^2) \;= \det\overline{\rho}_a \;;\quad \overline{r} = |\overline{\mathbf{r}}| \;= \sqrt{\overline{r}_1^2 + \overline{r}_2^2 + \overline{r}_3^2} \tag{16}$$

where in the respective JC , aJC models, the quantity $\mathcal{M}$, $\overline{\mathcal{M}}$, determines the departure from a pure state. We identify $\mathcal{M}$, $\overline{\mathcal{M}}$, as a *mixed state measure*. As comprehensively elaborated in [13], the mixed state measure can be defined as a composite of the various characteristic elements of measures of atomic state purity or entanglement. Here, we consider only two measures, the degree of purity $\mathcal{D}$ and the concurrence $\mathcal{C}$, noting that in [13], the degree of purity is defined in terms of a phase angle φ of the state purity measure complex amplitude in the form $\mathcal{D} = \tan\varphi$. The degree of purity and concurrence are connected by a complementarity relation

$$\mathcal{D}^2 + \mathcal{C}^2 = 1 \tag{17}$$

In the separate notations for JC and aJC models, the degree of purity and concurrence are obtained as [13]

$$\text{JC} \;:\quad \mathcal{D} = \sqrt{1 - \frac{4\det\rho_{\rm a}}{(\mathrm{Tr}\rho_{\rm a})^2}} \;= |\mathbf{r}| \;;\qquad \mathcal{C} = 2\sqrt{\det\rho_{\rm a}}$$

$$\text{aJC} \;:\quad \overline{\mathcal{D}} = \sqrt{1 - \frac{4\det\overline{\rho}_{\rm a}}{(\mathrm{Tr}\overline{\rho}_{\rm a})^2}} \;= |\overline{\mathbf{r}}| \;;\qquad \overline{\mathcal{C}} = 2\sqrt{\det\overline{\rho}_{\rm a}} \tag{18}$$

where the final form $\mathcal{D} = |\mathbf{r}|$, $\overline{\mathcal{D}} = |\overline{\mathbf{r}}|$, follows easily from substitution of the relations for $\det\rho_{\rm a}$, $\det\overline{\rho}_{\rm a}$ from equation (16) and the normalization $\mathrm{Tr}\rho_{\rm a} = 1$, $\mathrm{Tr}\overline{\rho}_{\rm a} = 1$ from equations (12) , (13). For normalized $\rho_a(t)$, $\overline{\rho}_a(t)$, the degree of purity and concurrence are seen to satisfy the complementarity relation in equation (17). Notice that for the normalized $\rho_a(t)$, $\overline{\rho}_a(t)$, the degree of purity equals the Bloch sphere radius $|\mathbf{r}|$, $|\overline{\mathbf{r}}|$, in the JC and aJC models.

According to the complementarity relation in equation (17), the time evolving degree of purity $\mathcal{D}$ and concurrence $\mathcal{C}$ alternately take complementary values within the range $\{0\ ,\ 1\}$, each having minimum value 0 and maximum value 1. When the degree of purity is at its maximum value $\mathcal{D} = 1$, the atom is in a completely disentangled pure state where the concurrence is at its minimum value $\mathcal{C} = 0$, while, on the other hand, when the degree of purity is at its minimum value $\mathcal{D} = 0$, the atom is in a totally mixed or maximally entangled state where the concurrence is at its maximum value $\mathcal{C} = 1$. Hence, the atomic state evolution is measured by the degree of purity and concurrence, such that at $(\mathcal{D} = 1\ ,\ \mathcal{C} = 0)$, the atom is in a completely disentangled pure state, while at $(\mathcal{D} = 0\ ,\ \mathcal{C} = 1)$, the atom is in a totally mixed or maximally entangled state. An interesting *uniformly mixed state* occurs when the degree of purity and concurrence are equal at $(\mathcal{D} = \frac{1}{\sqrt{2}}\ ,\ \mathcal{C} = \frac{1}{\sqrt{2}})$. We interpret the degree of purity and concurrence as the basic measures of the atomic state evolution.

3 Characterization of the dynamical evolution of the atomic state in the JC and aJC models

We can now use the atomic spin excitation number determined in equation (15) and the complementarity connected degree of purity and concurrence determined in equation (16), as the basic order parameters for studying the dynamical properties of the atom in the JC and aJC models. The atomic spin excitation number measures transitions between the qubit states signified by Rabi oscillations, while the degree of purity and concurrence measure the evolution of the atomic state characterized as pure, mixed or entangled.

In a useful departure from the arbitrariness of choices of physical parameters in earlier studies, we present a systematic characterization of the atomic state evolution using only the mean photon number amplitude $\sqrt{\overline{n}}$ of the coherent field mode and the dimensionless residual detuning parameters f, noting that the atom-field mode frequency detuning parameter k is fixed at $k = 1$ under resonance, but can be unified with $\sqrt{\overline{n}}$ and f as we introduce a property of *natural evolution* which essentially extends the form of resonance dynamics into the off-resonance regime.

3.1 Unifying parameters : natural evolution and a uniformly mixed state

To obtain a simple efficient characterization of the atomic state evolution in the JC and aJC dynamics as developed in this article, we unify the mean photon number amplitude $\sqrt{\overline{n}}$ and the residual detuning

parameter f by introducing simple linear relation in the form

$$f = \epsilon\sqrt{n}\ ; \quad \epsilon > 0 \tag{19}$$

where $\epsilon > 0$ is a numerical factor. This parameter unification now leaves the mean photon number amplitude $\sqrt{n}$ as the only variable physical control parameter, noting that the dimensionless atom-field mode frequency detuning parameter $k > 0$ is automatically fixed by the frequencies ω_0 , ω, where $k = 1$ specifies resonance, while $k \neq 1$ specifies off-resonance dynamics.

Substituting $f = \epsilon\sqrt{n}$ from equation (19) into the Rabi frequencies R_{n+j} , $\overline{R}_{n+j}$ and the related parameters in equation (10), evolution of the degree of purity $\mathcal{D}$ and concurrence $\mathcal{C}$ reveals a characteristic dynamical feature emerging at $\epsilon = 1$, which we identify as *natural evolution*, describing the dynamics of the atom in a *uniformly mixed state*, characterized by a symmetrical evolution of the degree of purity and concurrence about an axis passing through points where the degree of purity equals the concurrence, i.e., $\mathcal{D} = \mathcal{C}$-axis, defined as the *uniformly mixed state*-axis. Hence, taking into account the complementarity relation in equation (17), the general natural evolution property is defined together with the uniformly mixed state axis as

$$\begin{aligned} &\text{natural evolution property} \ : \quad \epsilon = 1\ ; \quad f = \sqrt{n} \\ &\text{Uniformly mixed state axis} \ : \quad \mathcal{D} = \mathcal{C} = \frac{1}{\sqrt{2}} \end{aligned} \tag{20}$$

In resonance dynamics where k is fixed at $k = 1$, the natural evolution property is defined as

$$\text{resonance natural evolution} \ : \quad k = 1\ ; \quad \epsilon = 1\ ; \quad f = \sqrt{n} \tag{21}$$

In defining natural evolution property in off-resonance $k \neq 1$ dynamics, we note that the larger aJC detuning parameter $\overline{\beta} = (k+1)f$ compared to the JC detuning parameter $\beta = (k-1)f$ means that, at a given value of the residual detuning parameter f, the dynamical evolution in the aJC model is generally faster than in the JC model. To synchronize the rates of dynamical evolution in the JC and aJC interaction mechanisms, the natural evolution property in off-resonance $k \neq 1$ dynamics is defined by setting the mean photon number amplitude $\sqrt{n}$ directly proportional to the product of k and f as

$$\text{off} - \text{resonance natural evolution} \ : \quad k \neq 1\ ; \quad \epsilon = 1\ ; \quad \sqrt{n} = \frac{1}{2}kf \quad \Rightarrow \quad f = \frac{2\sqrt{n}}{k} \tag{22}$$

The simple unifying relations in equations (20) , (21) , (22) show that the characteristic features of the atom-field mode dynamics are determined only by α, as clarified in the discussion in sections 3.2 , 3.3 below. Notice that the resonance natural evolution property in equation (21) effectively defines $\sqrt{n} = \frac{\omega}{\lambda}$ (in terms of the field mode frequency ω as in [5]), while the off-resonance natural evolution property in equation (22) effectively defines $\sqrt{n} = \frac{1}{2}\frac{\omega_0}{\lambda}$ (in terms of the atomic state transition frequency ω_0). In describing the characteristic features of natural evolution according to the atom-field mode coupling strengths in resonance or off-resonance dynamics in the JC and aJC models, we apply the property that strong coupling interaction is determined by the residual detuning parameter $f > 0$ in the small value range $0 < f < 1$, while weak coupling interaction is determined by the large value range $f > 1$ (i.e., $1 < f < \infty$).

In general, natural evolution of the atomic state is a beautiful stable dynamical process composed of well defined atomic state regimes in resonance $k = 1$ and off-resonance $k \neq 1$. In particular, in resonance $k = 1$ dynamics, natural evolution in the strong coupling $0 < f < 1$ region is composed of a *ground state regime* within the mean photon number amplitude range $0 < \sqrt{n} = f \leq 0.1$ and a *mixed state regime* within the range $0.1 < \sqrt{n} = f < 1$, while in the weak coupling $f > 1$ $(1 < f < \infty)$ region, natural evolution is composed of a *reversible mixed state regime* within the range $1 < \sqrt{n} = f \leq 8.55$, an *irreversible mixed state regime* within the range $8.55 < \sqrt{n} = f \leq 9.2$, a *reversible entangled state regime* within the range $9.2 < \sqrt{n} = f \leq 9.57$ and an *irreversible entangled state regime* within the range $9.57 < \sqrt{n} = f < 11.2$. A *maximally entangled state regime* occurring at $\sqrt{n} \geq 11.2$ is completely independent of the detuning parameters $k > 0$, $f > 0$. Similar characteristic atomic state evolution regimes also occur in off-resonance $k \neq 1$ natural evolution, but now the general nature is determined also by $k \neq 1$ in the small value range $0 < k < 1$ or large value range $k > 1$.

We interpret the natural evolution property at $\epsilon = 1$, $\sqrt{n} = f$ under resonance $k = 1$ and $\sqrt{n} = \frac{k}{2}f$ off-resonance $\neq 1$, as the optimal dynamics of the system in a uniformly mixed state over the entire strong coupling $0 < f < 1$ and weak coupling $f > 1$ ranges of the JC and aJC models. The natural evolution

property essentially generalizes the characteristic features of resonance dynamics to include off-resonance dynamics. Characterization of the atomic state evolution, revealing general features of the dynamics, then begins from the uniformly mixed state in natural evolution, determined by keeping the mean photon number amplitude fixed at the natural evolution value, while varying the residual or atom-field mode frequency detuning parameter f , k to larger or smaller values as appropriate. In this respect, we note that in the strong coupling region where the residual detuning parameter is restricted within the small value range $0 < f < 1$, only the mean photon number amplitude is increased to larger values, up to a maximum value $\sqrt{\overline{n}}_{max} = 11.2$, where the concurrence and degree of purity reach their respective steady state time-independent maximum and minimum values ($\sqrt{\overline{n}} = 11.2 : \quad \mathcal{C} = 1 \ , \ \mathcal{D} = 0$), signifying a maximally entangled state. The onset of the maximally entangled state at $\sqrt{\overline{n}} = 11.2$ applies generally in both strong and weak coupling interactions. This maximally entangled state describes steady state time-independent evolution which does not change with further increases $\sqrt{\overline{n}} > 11.2$ and is completely independent of the detuning parameters over the entire ranges $f > 0$, $k > 0$.

Generally, in both resonance and off-resonance JC and aJC dynamics, increasing the mean photon number amplitude $\sqrt{\overline{n}}$ raises the concurrence towards its steady state time-independent maximum value $\mathcal{C} = 1$, but lowers the degree of purity towards the corresponding minimum value $\mathcal{D} = 0$ at $\sqrt{\overline{n}} \geq 11.2$, where the state is maximally entangled. On the other hand, in resonance $k = 1$ dynamics, increasing the residual detuning parameter f within the various state evolution regimes raises the degree of purity towards the respective steady state time-independent maximum values $\mathcal{D}_{max} \leq 1$, but lowers the concurrence towards the corresponding minimum values $\mathcal{C}_{min} \geq 0$ at appropriate critical values $f_c >> 1$; similar pattern of evolution occurs in off-resonance $k \neq 1$ on decreasing k to lower values $k < 1$. We note that under resonance $k = 1$, the JC dynamics, which is completely independent of the residual detuning parameter f, cannot achieve a steady state time-independent evolution. Hence, in resonance $k = 1$ dynamics, increasing f affects only the atomic state evolution in the aJC model, which achieves steady state time-independent evolution at critical values $f_c >> 1$. However, in off-resonance $k \neq 1$ dynamics, varying f affects atomic state evolution in both JC and aJC models, leading to the property that off-resonance JC dynamics can achieve steady state time-independent evolution.

In an interpretation, (i) increasing the mean photon number amplitude $\sqrt{\overline{n}}$ drives the atomic state towards the maximally entangled state (ii) the growth of the degree of purity towards the steady state time-independent maximum value $\mathcal{D} = 1$, with the concurrence falling towards the corresponding minimum value $\mathcal{C} = 0$ signifies evolution of the atomic state towards a completely disentangled pure state, while the growth of the concurrence towards the steady state time-independent maximum value $\mathcal{C} = 1$, with the degree of purity falling towards the corresponding minimum value $\mathcal{D} = 0$ signifies evolution of the atomic state towards a maximally entangled state; on increasing the residual detuning parameter f or decreasing the atom-field mode frequency detuning parameter k in the aJC model and in off-resonance JC model, the dynamics progresses through intermediate mixed or entangled states describing periodic evolution, developing towards steady state time-independent evolution in a completely disentangled pure state or stable mixed state or stable entangled state; we emphasize that resonance JC dynamics cannot reach a steady state time-independent evolution (iii) the evolution of the spin excitation number with increasing $\sqrt{\overline{n}}$, f, or decreasing/increasing k, essentially measures transitions characterized by Rabi oscillations between the qubit states.

We have established that the maximally entangled state also emerges naturally in evolution over a long interaction time, where the concurrence grows asymptotically towards the steady state time-independent maximum value 1, while the degree of purity decays asymptotically towards the corresponding minimum value 0 over increasing interaction time. After some time $t_c > 0$ within the long interaction time, the concurrence and degree of purity reach and remain at their respective steady state time-independent maximum and minimum values ($\mathcal{C} = 1 \ , \ \mathcal{D} = 0$), where the atom now remains in a stable maximally entangled state.

Considering resonance $k = 1$ dynamics, we study the natural evolution of the atomic state and Rabi oscillations between the qubit states determined by $0 < \sqrt{\overline{n}} = f < 1$ in the strong coupling and $\sqrt{\overline{n}} = f > 1$ ($1 < \sqrt{\overline{n}} = f < \infty$) in the weak coupling JC and aJC models in sections 3.2 below. In the strong coupling dynamics in section 3.2.1, we keep the residual aJC detuning parameter f fixed in the range $0 < f < 1$, but progressively increase the mean photon number amplitude $\sqrt{\overline{n}}$ to study the development of the natural evolution of the atomic state into a time-independent completely disentangled pure state or maximally entangled state, while in the weak coupling dynamics in section 3.2.2, we study the same process by progressively increasing either the mean photon number amplitude or the residual detuning parameter f, keeping the other fixed in each case. We present off-resonance $k \neq 1$ dynamics in section 3.3, followed by a beautiful formulation of resonance $k = 1$ intermediate coupling $f = 1$ interaction, developed as a

spin-displaced field mode with an exact eigenstate spectrum, in section 3.4.

3.2 Resonance dynamics

In standard studies of the JC model, the resonance condition $\omega = \omega_0$ $(k = 1)$ is applied to obtain an optimal dynamical evolution characterized by an exact exchange of energy between the atom and field mode, one emitting and the other absorbing, the same amount of energy ($\hbar\omega = \hbar\omega_0$). In this article, we use the degree of purity, concurrence and spin excitation number to present a fairly more general study of resonance dynamics characterized by $k = 1$ in both JC and aJC models.

The resonance $k = 1$ condition specified in equation (9) shows that the dimensionless JC detuning parameter vanishes as $\beta = 0$, but the aJC remains detuned by the non-vanishing residual detuning parameter as $\overline{\beta} = 2f > 0$. The resonant JC dynamics is thus driven only by the mean photon number amplitude $\sqrt{\overline{n}}$, while the resonant aJC dynamics is driven by both $\sqrt{\overline{n}}$ and f. Specifically, in the resonance dynamics, setting $k = 1$ in equation (10) gives Rabi frequencies and related interaction parameters in the resonant JC and aJC models in the form

$$k = 1$$

$$\text{JC} \;:\quad R_{n+j} = \lambda\sqrt{n+j}\;; \qquad c_{n+j} = 0\;; \qquad s_{n+j} = 1$$

$$\text{aJC} \;:\quad \overline{R}_{n+j} = \lambda\sqrt{n+j+f^2}\;; \qquad \overline{c}_{n+j} = \frac{f}{\sqrt{n+j+f^2}}\;; \qquad \overline{s}_{n+j} = \frac{\sqrt{n+j}}{\sqrt{n+j+f^2}}\;; \quad j = 0, 1 \tag{23}$$

For effective characterization of the atomic state, we apply the resonance natural evolution property from equation (21) in equation (23) according to

$$k = 1\;; \quad \epsilon = 1\;; \quad f = \sqrt{\overline{n}} \tag{21$'$}$$

We immediately see a distinct difference between the JC and aJC interaction mechanisms in resonance $k = 1$ dynamics. The resonant JC Rabi frequency and related interaction parameters R_{n+j} , c_{n+j} , s_{n+j} in equation (23) are completely independent of the residual detuning parameter f, while the corresponding aJC Rabi frequency and related interaction parameters $\overline{R}_{n+j}$, $\overline{c}_{n+j}$, $\overline{s}_{n+j}$ are intrinsically dependent on the parameter f. The atomic state evolution in the resonant JC model is therefore characterized only by the mean photon number amplitude $\sqrt{\overline{n}}$ in the photon distribution probability amplitudes $\sqrt{P_{n+j}}$, while the evolution in the resonant aJC model is characterized by both $\sqrt{\overline{n}}$ in the photon distribution probability amplitudes and the residual detuning parameter f defining the Rabi frequency and related interaction parameters. In the resonance natural evolution property in equation (21$'$), the resonant JC dynamics, driven only by $\sqrt{\overline{n}}$, remains the same, unaffected by $f > 0$, throughout the strong interaction $0 < f < 1$ and the weak interaction $1 < f < \infty$ regimes, while the corresponding resonant aJC dynamics, driven by both $\sqrt{\overline{n}}$ and f, is characterized by the interesting detailed features of natural evolution property $f = \sqrt{\overline{n}}$ described by a uniformly mixed atomic state, which develops into steady state time-independent evolution on increasing the residual detuning parameter from the natural evolution value $f = \sqrt{\overline{n}}$ to larger critical values $f_c = \epsilon_c\sqrt{\overline{n}}$, $\epsilon_c >> 1$, where the atom is in a completely disentangled pure state or stable mixed state or stable entangled state. In the resonant JC dynamics, the atomic state can evolve only into a short-lived nearly pure state in the middle of the collapse period of the spin excitation number within a state evolution regime specified by $\sqrt{\overline{n}} \leq 8.55$, but cannot develop into a steady state time-independent evolution, except at the critical value $\sqrt{\overline{n}_c} = 11.2$ where the evolution reaches the maximally entangled state in both JC and aJC models.

3.2.1 Atomic state evolution in the resonant strong coupling interaction : $k = 1\;;\; 0 < f < 1$

As defined above, the strong coupling interaction is characterized by the residual detuning parameter f in the range $0 < f < 1$. In the resonant strong coupling JC and aJC models, the natural evolution property of the atomic state in equation (21$'$) is set by

$$k = 1\;; \qquad f = \sqrt{\overline{n}} \quad \Rightarrow \quad 0 < f = \sqrt{\overline{n}} < 1 \tag{24}$$

meaning that resonance natural evolution in the strong coupling regime is characterized by both residual detuning parameter f and mean photon number amplitude $\sqrt{\overline{n}}$ in the small value range $0 < f = \sqrt{\overline{n}} < 1$, which we now describe.

Setting $f = \sqrt{\overline{n}}$ in equation (23) and substituting the respective Rabi frequencies and related interaction parameters into the corresponding Bloch radius components obtained in equations (7) , (12) , (13), we determine explicit time evolving forms of the respective spin excitation numbers $\langle\sigma_+\sigma_-\rangle$, $\langle\sigma_-\sigma_+\rangle$, degree of purity $\mathcal{D}$, $\overline{\mathcal{D}}$ and concurrence $\mathcal{C}$, $\overline{\mathcal{C}}$ defined in equations (15) and (18), noting the complementarity relation $\mathcal{C} = \sqrt{1-\mathcal{D}^2}$ in equation (17). For $\sqrt{\overline{n}} = f$ in the range $0 < \sqrt{\overline{n}} = f < 1$, we have plotted the degree of purity, concurrence and spin excitation number over scaled time $\tau = \lambda t$ to determine the natural evolution of the atomic state in the resonant strong coupling JC model in Fig.1 , Fig.3 and aJC model in Fig.2 , Fig.4. In the plots, we have identified the degree of purity, concurrence and spin excitation number collectively as state quantifiers, but distinguished them by colors as appropriate.

The natural evolution of the atomic state in the resonant strong coupling JC and aJC models is composed of two distinct dynamical regimes. The first regime occurs in the parameter range $0 < \sqrt{\overline{n}} = f \leq 0.1$, which we have identified as the *ground state evolution* regime, plotted over scaled time $\tau = \lambda t$ in Fig.1 in the JC model and Fig.2 in the aJC model. The second regime occurs in the parameter range $0.1 < \sqrt{\overline{n}} = f < 1$, which we have identified as the *mixed state evolution* regime, plotted in Fig.3 in the JC model and Fig.4 in the aJC model.

In each Figure throughout the text, we have provided the uniformly mixed state-axis passing through points where the degree of purity and concurrence have equal values $\mathcal{D} = \mathcal{C} = \frac{1}{\sqrt{2}}$.

A. Ground state evolution regime : $0 < \sqrt{\overline{n}} = f \leq 0.1$

The ground state evolution regime is characterized by small mean photon number amplitude $\sqrt{\overline{n}}$ within the range $0 < \sqrt{\overline{n}} \leq 0.1$ where the initial field mode is strictly in the vacuum state $|0\rangle$ and the coherent state $|\alpha\rangle$ ($\alpha \equiv \sqrt{\overline{n}}$) expansion contains only the vacuum state. Hence, in the small mean photon number amplitude $\sqrt{\overline{n}}$ range $0 < \sqrt{\overline{n}} < 0.1$, the expansion of the atom-field initial state in equation (4) contains only the ground state $|\psi_{g\alpha}\rangle = |g0\rangle$.

We have plotted the ground state evolution in the resonant strong coupling JC model in Fig.1. The

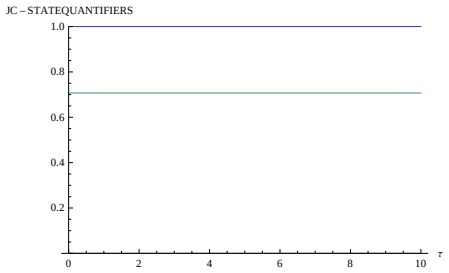

Figure 1: Natural evolution of degree of atomic state purity $\mathcal{D}$ (BLUE), concurrence $\mathcal{C}$ (RED-not visible at minimum value 0 exactly along τ-axis) and excitation number $\langle\sigma_+\sigma_-\rangle$ (GREEN-not visible at minimum value 0 exactly along τ-axis) in the resonant strong coupling JC model at $k = 1$; $\sqrt{\overline{n}} = f = 0.015$ (within the ground state evolution regime $0 < \sqrt{\overline{n}} = f \leq 0.1$) over scaled time $\tau = \lambda t$

evolution in Fig.1 reveals that, within the ground state evolution regime $0 < \sqrt{\overline{n}} = f \leq 0.1$ in the resonant strong coupling JC model, the atomic state remains a completely disentangled pure state where the degree of purity (blue) is at the time-independent maximum value $\mathcal{D} = 1$, while the concurrence (red-not clearly visible along the time τ-axis) and spin excitation number (yellow-not clearly visible along the time τ-axis) are both at their time-independent minimum values ($\mathcal{C} = 0$, $\langle\sigma_+\sigma_-\rangle = 0$).

To account for the form of natural evolution in Fig.1 in the JC model, we note that the ground state $|g0\rangle$ is an eigenstate of the JC Hamiltonian H_{JC} in equation (3) [2 , 17]. Hence, the JC interaction does not cause transitions from the initial state $|\psi_{g\alpha}\rangle = |g0\rangle$, but generates only a plane wave evolution according to

$$\hat{N}|g0\rangle = -\frac{1}{2}|g0\rangle \ ; \qquad \hat{R}|g0\rangle = -\frac{1}{2}(\omega_0 - \omega)|g0\rangle \quad \Rightarrow \quad |\Psi_{JC}(t)\rangle = e^{\frac{i}{2}\omega_0 t}|g0\rangle \tag{25}$$

This plane wave is a separable pure state $|\Psi_{JC}(t)\rangle = e^{\frac{i}{2}\omega_0 t}|g\rangle|0\rangle$ of the atom and field mode ground states, where it is easily established that the atomic spin excitation number is 0, the degree of purity is exactly at the maximum value 1 and the concurrence exactly at its minimum value 0, as Fig.1 shows. This signifies the property that within the ground state evolution regime $0 < \sqrt{\overline{n}} = f < 1$ of the resonant strong coupling JC

model, the atom remains in a pure state, essentially its time evolving ground state $e^{\frac{i}{2}\omega_0 t}|g\rangle$. This explains the time-independent degree of purity at maximum value 1, concurrence and spin excitation number at minimum values 0 in Fig.1.

We have plotted the ground state evolution in the resonant strong coupling aJC model in Fig.2.

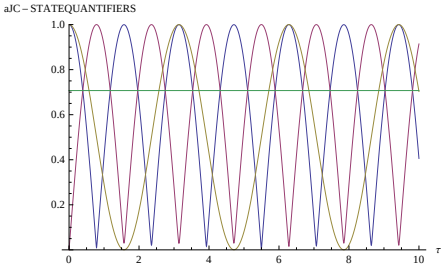

Figure 2: Natural evolution of degree of atomic state purity $\overline{\mathcal{D}}$ (BLUE), concurrence $\overline{\mathcal{C}}$ (RED) and excitation number $\langle\sigma_-\sigma_+\rangle$ (YELLOW) in the resonant strong coupling aJC model at $k = 1$; $\sqrt{\overline{n}} = f = 0.015$ (within the ground state evolution regime $0 < \sqrt{\overline{n}} = f \leq 0.1$) over scaled time $\tau = \lambda t$

The evolution in Fig.2 reveals that, within the ground state evolution regime $0 < \sqrt{\overline{n}} = f \leq 0.1$ in resonant strong coupling aJC model, the atomic state is characterized by perfect Rabi oscillations of the degree of purity (blue) , concurrence (red) and spin excitation number (yellow). The interesting features of the Rabi oscillations in Fig.2 are (i) the degree of purity and concurrence undergo alternate Rabi oscillations of *equal period* between their maximum and minimum values $\{1\ ,\ 0\}$ in opposite sense, one rising, the other falling, and vice-versa, signifying the property that within the ground state evolution regime $0 < \sqrt{\overline{n}} = f \leq 0.1$ of the resonant strong coupling aJC model, the atomic state alternately evolves periodically between a completely disentangled pure state and a maximally entangled state (ii) the degree of purity and concurrence cross at points on the uniformly mixed state axis (green-axis) where $\overline{\mathcal{D}} = \overline{\mathcal{C}} = \frac{1}{\sqrt{2}}$ (iii) the period of Rabi oscillations of the spin excitation number is *double* the equal periods of Rabi oscillations of the degree of purity and concurrence (iv) the maximum of the spin excitation number coincides with the maximum of the degree of purity, while the minimum of the spin excitation number coincides with the minimum of the concurrence, each after every two periods of oscillations of the degree of purity and concurrence (iv) the dynamical property that the evolution of the spin excitation number begins from the maximum value $\langle\sigma_-\sigma_+\rangle = 1$ at initial time $\tau = 0$ signifies a fundamental quantum mechanical phenomenon that the ground state $|g0\rangle$ in the aJC model is excited.

To account for the perfect periodic Rabi oscillations in Fig.2 in the aJC model, we note that the ground state $|g0\rangle$ is a qubit state of the aJC Hamiltonian H_{aJC} in equation (3) [2], with qubit state transitions and general time evolving state vector obtained in the general form

$$\hat{\overline{N}}|g0\rangle = \frac{3}{2}|g0\rangle\ ;\quad \hat{\overline{R}}|g0\rangle = \overline{R}_0|\ \overline{\phi}_{g0}\rangle\ ;\quad |\ \overline{\phi}_{g0}\rangle = -\overline{c}_0|g0\rangle + \overline{s}_0|e1\rangle\ ;\quad \overline{R}_0 = \lambda\sqrt{1+\frac{1}{4}(k+1)^2 f^2}$$

$$\overline{c}_0 = \frac{(k+1)f}{2\sqrt{1+\frac{1}{4}(k+1)^2 f^2}}\ ;\qquad \overline{s}_0 = \frac{1}{\sqrt{1+\frac{1}{4}(k+1)^2 f^2}}$$

$$|\Psi_{aJC}(t)\rangle = e^{-\frac{3}{2}i\omega t}\left((\cos(\ \overline{R}_0 t) + i\ \overline{c}_0 \sin(\ \overline{R}_0 t))|g0\rangle - i\ \overline{s}_0 \sin(\ \overline{R}_0 t)|e1\rangle\right) \tag{26}$$

Setting the resonance value $k = 1$ in $\overline{R}_0$, $\overline{c}_0$, $\overline{s}_0$ and applying an approximation $1 >> f$ within the ground state evolution range $0 < \sqrt{\overline{n}} = f \leq 0.1$ gives

$$k = 1\ ;\quad f << 1\quad \Rightarrow\quad \overline{R}_0 \approx \lambda\ ;\qquad \overline{c}_0 \approx 0\ ;\qquad \overline{s}_0 \approx 1$$

$$|\Psi_{aJC}(t)\rangle \approx e^{-\frac{3}{2}i\omega t}\left(\cos(\ \lambda t)|g0\rangle - i\sin(\ \lambda t)|e1\rangle\right) \tag{27}$$

which describes periodic blue-sideband transitions between the ground state $|g0\rangle$ and the one-photon excited state $|e1\rangle$ at Rabi oscillation frequency $\overline{R}_0 = \lambda$. The precise periodic evolution described by the time evolving aJC state vector $|\Psi_{aJC}(t) >$ in equation (27) explains the perfect periodic Rabi oscillations between maximum and minimum values $\{1\ ,\ 0\}$ of the degree of purity (blue), concurrence (red) and spin excitation

number (yellow) in Fig.2, showing that natural evolution within the ground state regime $0 < \sqrt{\overline{n}} = f \leq 0.1$ in resonant strong coupling aJC interaction describes the atomic state spontaneously evolving alternately between short-lived (sharp maxima and minima) completely disentangled pure and maximally entangled states.

We observe that the elimination of the residual detuning parameter f through the approximation in equation (27) reveals the important property that the Rabi oscillations of the spin excitation number, in particular, and of the degree of purity and concurrence, within the ground state evolution regime, are internal dynamical properties of the blue-sideband transitions generated by the aJC interaction mechanism, which we have explained in physical terms in [1].

We consider that the blue-sideband ground state excitation and qubit transitions generated by the aJC interaction mechanism according to equation (27) may be the underlying dynamical phenomenon of ground state excitation observed in deep strong coupling regime in the quantum Rabi model in [5] and related studies cited therein. Here, we note that the JC interaction component does not cause ground state excitations, but only generates free ground state evolution according to equation (25), which we have established as a general property in resonance and off-resonance dynamics in [2].

B. Mixed state evolution regime : $0.1 < \sqrt{\overline{n}} = f < 1$

The mixed state evolution regime is characterized by small parameter $\sqrt{\overline{n}}$, f values in the range $0.1 < \sqrt{\overline{n}} = f < 1$. The mean photon number amplitude $\sqrt{\overline{n}}$ within the range $0.1 < \sqrt{\overline{n}} < 1$ seems to activate all low-lying qubit states $|g0\rangle$, $|g1\rangle$, $|g2\rangle$, in the atom-field initial state $|\psi_{g\alpha}\rangle$ ($\alpha \equiv \sqrt{\overline{n}}$) in equation (4). In this case, both JC and aJC Hamiltonians H_{JC} , H_{aJC} in equation (3) generate qubit state transitions described by respective time evolving state vectors $|\Psi_{JC}\rangle$, $|\Psi_{aJC}(t)\rangle$ in the general form in equations (12) , (13), but the expansion over photon numbers $n = 0, 1, 2, ...$, now includes only the few active low-lying qubit states. This explains the form of natural evolution which we have identified as a mixed state evolution regime determined by the parameter range $0.1 < \sqrt{\overline{n}} = f < 1$, shown in Fig.3 in the JC model and Fig.4 in the aJC model.

The fairly irregular natural evolution in Fig.3 shows that in the mixed state evolution regime $0.1 < \sqrt{\overline{n}} = f < 1$ in resonant strong coupling JC model, the atomic state spontaneously evolves to a very nearly disentangled pure state at the scaled times $\tau_p = \lambda t_p$ where the degree of purity (blue) very nearly reaches the maximum value $\mathcal{D} \approx 1$, with corresponding concurrence (red) minimum value at $\mathcal{C} < 0.1$.

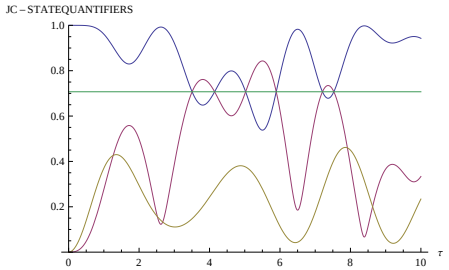

Figure 3: Natural evolution of degree of atomic state purity $\mathcal{D}$ (BLUE), concurrence $\mathcal{C}$ (RED) and spin excitation number $\langle \sigma_+ \sigma_- \rangle$ (YELLOW) in the resonant strong coupling JC model at $k = 1$; $\sqrt{\overline{n}} = f = 0.8$ (within the mixed state evolution regime $0.1 < \sqrt{\overline{n}} = f < 1$) over scaled time $\tau = \lambda t$

The property that the spin excitation number $< \sigma_+ \sigma_- >$ (yellow) in Fig.3 evolves above the 0 value provides direct evidence of qubit state transitions generated by the JC interaction in the mixed state evolution regime $0.1 < \sqrt{\overline{n}} = f < 1$, thus confirming the activation of low-lying qubit states $|g1\rangle$, $|g2\rangle$, etc, above the ground state $|g0\rangle$.

The fairly regular natural evolution with oscillations about the uniformly mixed state axis (green-axis) in Fig.4 shows that in the mixed state evolution regime $0.1 < \sqrt{\overline{n}} = f < 1$ in resonant strong coupling aJC model, the atomic state is fairly uniformly mixed, with concurrence (red) generally evolving above the uniformly mixed state axis signifying a tendency of evolution towards an entangled state at scaled times $\tau_{en} = \lambda t_{en}$ where the concurrence evolves to a maximum value $\mathcal{C} \approx 0.9$, fairly close to the maximum value 1 for a maximally entangled state, with corresponding degree of purity (blue) minimum value at $\mathcal{D} < 0.45$.

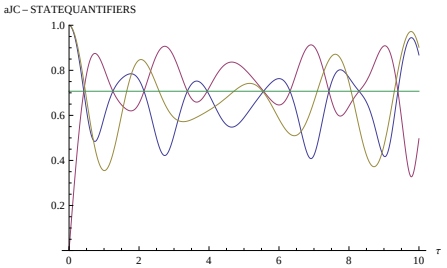

Figure 4: Natural evolution of degree of atomic state purity $\mathcal{D}$ (BLUE), concurrence $\mathcal{C}$ (RED) and spin excitation number $\langle\sigma_-\sigma_+\rangle$ (YELLOW) in the resonant strong coupling aJC model at $k = 1$; $\sqrt{\overline{n}} = f = 0.8$ (within the mixed state evolution regime $0.1 < \sqrt{\overline{n}} = f < 1$) over scaled time $\tau = \lambda t$

The diminishing of the spin excitation number (yellow) undergoing slow damped evolution in Fig.4 is possibly due to interference among transitions of the increased number of active low-lying qubit states $|g0\rangle$, $|g1\rangle$, $|g2\rangle$, etc, within the mixed state evolution regime $0.1 < \sqrt{\overline{n}} = f < 1$, compared to the perfect Rabi oscillations of the spin excitation number in the ground state evolution regime $0 < \sqrt{\overline{n}} = f < 1$ in Fig.2, where only the ground state qubit $|g0\rangle$ is active.

C. Increasing $\sqrt{\overline{n}}$: emergence of collapses, revivals, pure and entangled state evolution

We now study the dynamics of atomic state evolution beyond natural evolution at $0 < \sqrt{\overline{n}} = f < 1$ in the resonant strong coupling JC and aJC models, by increasing either of the parameters $\sqrt{\overline{n}}$, f, while keeping the other fixed at the specified natural evolution value. Here, the property that the resonant JC model is completely independent of the residual detuning parameter f according to equation (23), together with the property that f is restricted within the small value range $0 < f < 1$ in the strong coupling interactions, means that only the mean photon number amplitude $\sqrt{\overline{n}}$ remains a free parameter which can be increased to larger values $\sqrt{\overline{n}} > 1$. We have therefore kept f fixed within the strong coupling range $0 < f < 1$, but progressively increased $\sqrt{\overline{n}}$ to larger values to study the dynamics of the atomic state beyond the natural evolution at $0 < \sqrt{\overline{n}} = f < 1$.

From the onset, we consider that, according to the definition of the photon distribution probability P_{n+j}, $j = 0, 1, -1$, in equation (7), increasing the mean photon number amplitude $\sqrt{\overline{n}}$ effectively increases the probability of occupation of higher excited field mode number states $|n\rangle$. Hence, increasing $\sqrt{\overline{n}}$ generally increases the number of atom-field mode qubit states $|gn\rangle$ included in the expansion of the initial state $|\psi_{g\alpha}\rangle$ in equation (4). The underlying physical consequence is that the interference among the transitions generated by the JC or aJC interaction mechanism in a superposition of an increasing number of qubit states $|gn\rangle$, $n = 0, 1, 2, 3, ..., \infty$, effectively drives the system to a generally mixed state as the mean photon number amplitude $\sqrt{\overline{n}}$ is increased to large values. The expected net effect is that increasing $\sqrt{\overline{n}}$ leads to an increase in the concurrence which measures the mixed state or entanglement property, a corresponding decrease in the degree of purity which measures the pure state property and a decrease or diminishing of the spin excitation number due to the destructive interference of a large number of qubit transitions.

Indeed, we have established that, increasing the mean photon number amplitude to larger values $\sqrt{\overline{n}} > 1$ raises the concurrence $\mathcal{C}$ towards its maximum value 1, but lowers both the degree of purity $\mathcal{D}$ and spin excitation number $\langle\sigma_\pm\sigma_\mp\rangle$ towards their respective minimum values 0 in both JC and aJC models. A very important property which emerges is that, $\sqrt{\overline{n}}$ cannot be increased to arbitrarily large values, but only up to a well defined maximum value $\sqrt{\overline{n}_{max}} = 11.2$, where the atomic state evolution reaches the maximally entangled state, which becomes clear below.

As $\sqrt{\overline{n}}$ is increased from the natural evolution values $0 < \sqrt{\overline{n}} < 1$, the general mixed state property emerges prominently. Within the range of values $1 < \sqrt{\overline{n}} \leq 9.72$, the degree of purity, concurrence and spin excitation number, each develops evolution with collapses and revivals, where the maximum and minimum values of the degree of purity or concurrence are generally below, respectively, above, the expected completely disentangled pure state or maximally entangled state values 1 or 0. The *optimal* characteristic feature of this evolution with collapses and revivals is achieved at the value $\sqrt{\overline{n}} = 7$, plotted in Fig.5 in the JC model and in Fig.6 in the aJC model, where the degree of purity (blue) spontaneously rises sharply to a short-lived maximum value $\mathcal{D} \approx 1$, very very close to maximum value 1 for a completely disentangled pure state and the corresponding concurrence (red) spontaneously falls sharply to a short-lived minimum value $\mathcal{C} \approx 0.125$,

very close to the minimum value 0, in the middle of the first collapse period of the spin excitation number. Note that the approximate maximum and minimum values ($\mathcal{D} \approx 1$, $\mathcal{C} \approx 0.125$) in both JC and aJC models must satisfy the complementarity relation in equation (17).

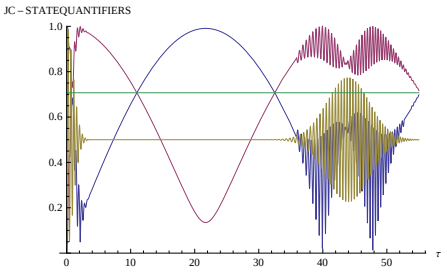

Figure 5: Resonance evolution of degree of atomic state purity $\mathcal{D}$ (BLUE), concurrence $\mathcal{C}$ (RED) and spin excitation number $\langle \sigma_+ \sigma_- \rangle$ (YELLOW) in the strong coupling JC model at $k = 1$; $\sqrt{\overline{n}} = 7$; $0 < f < 1$ over scaled time $\tau = \lambda t$

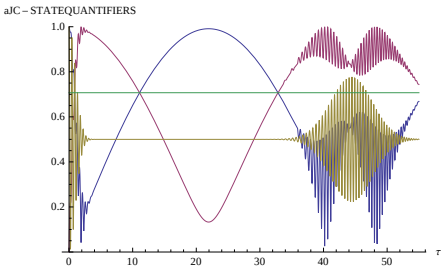

Figure 6: Resonance evolution of degree of atomic state purity $\overline{\mathcal{D}}$ (BLUE), concurrence $\overline{\mathcal{C}}$ (RED) and spin excitation number $\langle \sigma_- \sigma_+ \rangle$ (YELLOW) in the strong coupling aJC model at $k = 1$; $\sqrt{\overline{n}} = 7$; $0 < f < 1$ over scaled time $\tau = \lambda t$

Notice that in the evolution in both JC and aJC models in Fig.5 , Fig.6, the degree of purity (blue) and concurrence (red) cross at points on the uniformly mixed state axis (green), thereby fulfilling the complementarity relation in equation (17), while the spin excitation number (yellow) undergoes collapses and revivals about the $\frac{1}{2}$-axis, at half the maximum value 1, which we may identify as the *resonance spin excitation number collapse*-axis as a reference for the evolving spin excitation number. Note that, according to the definitions of the respective JC and aJC spin excitation numbers $\langle \sigma_+ \sigma_- \rangle = \frac{1}{2}(1 + r_3)$, $\langle \sigma_- \sigma_+ \rangle = \frac{1}{2}(1 - \overline{r}_3)$ in equation (15), the resonance spin excitation collapse axis passes through points where the respective state population inversion vanishes as $r_3 = 0$, $\overline{r}_3 = 0$.

The similarity of the evolution in Fig.5 in the JC model and Fig.6 in the aJC model is due to the property that at the larger value $\sqrt{\overline{n}} = 7$, dynamical effects of the small aJC residual detuning parameter $\overline{\beta} = 2f$ in the strong coupling range $0 < f < 1$, do not change the dynamics significantly compared to the resonant JC dynamics with vanishing detuning parameter $\beta = 0$. In particular, for photon excitation numbers $n \geq 1$ arising in the superposition of qubit states $|gn\rangle$ at large $\sqrt{\overline{n}} > 1$, the approximation $f << 1$ applied within the ground state evolution regime in equation (27), affecting only the aJC model in resonance $k = 1$, can be generalized to the evolution at large $\sqrt{\overline{n}} > 1$ to obtain the effective JC and aJC Rabi oscillation frequencies and the related interaction parameters in equation (10), together with the respective approximate general time evolving state vector in resonance $k = 1$ in the form

$$k = 1 \; ; \quad n \geq 0 \; ; \quad j = 0, 1 \; ; \quad \sqrt{n + j} >> f$$

$$\overline{R}_{n+j} \approx R_{n+j} = \lambda \sqrt{n + j} \; ; \quad \overline{c}_{n+j} \approx c_{n+j} = 0 \; ; \quad \overline{s}_{n+j} \approx s_{n+j} = 1$$

$$|\Psi_{JC}(t)\rangle = \sum_{n=0}^{\infty} (\sqrt{P_n} e^{-i\omega n t} (\cos(\lambda \sqrt{n} t) |g\rangle - i \sqrt{P_{n+1}} e^{-i\omega(n+1)t} \sin(\lambda \sqrt{n+1} t) |e\rangle) |n\rangle$$

$$|\Psi_{aJC}(t)\rangle \approx \sum_{n=0}^{\infty}(\sqrt{P_n}e^{-i\omega(n+1)t}(\cos(\lambda\sqrt{n+1}t)|g\rangle - i\ \sqrt{P_{n-1}}e^{-i\omega nt}\sin(\lambda\sqrt{n}t)|e\rangle\ )|n\rangle \qquad (28)$$

noting that in the resonance $k = 1$ dynamics, the JC results in equation (28) are exact, agreeing with equation (23). Notice that the approximate form of the resonant aJC state vector $|\Psi_{aJC}(t)\rangle$ in equation (28) is precisely similar to the exact resonant JC state vector $|\Psi_{JC}(t)$, the two differing only in the interchange of field mode excitation numbers $n \rightleftharpoons n+1$ in the Rabi frequencies and global time evolving phase factors, which explains the similarity in the forms of dynamical evolution in the resonant strong coupling JC and aJC models in Fig.5 and Fig.6.

We observe that, the phenomenon in which the atomic state spontaneously evolves to an approximately disentangled pure state signified by maximum degree of purity $\mathcal{D} \approx 1$ and minimum concurrence $\mathcal{C} \approx 0.125$ at the middle of the first collapse period of the spin excitation number (or spin population inversion) was first determined in resonant JC model precisely in the same form at $\overline{n} = 49$ ($\sqrt{\overline{n}} = 7$) as in Fig.5 by Gea-Banacloche using the atomic state purity measure $Tr\hat{\rho}_a^2$ in [6] and a little later by Phoenix and Knight using the von Newman entropy as a measure of the atomic state entanglement in [9].

In this article, we continue applying the qualitative approach to determine the dynamical properties of the atomic state evolution by keeping detuning fixed in the strong coupling range $0 < f < 1$, while increasing the mean photon number amplitude to larger values $\sqrt{\overline{n}} > 7$. We re-emphasize that for all values $\sqrt{\overline{n}} \neq 7$ in the range $1 < \sqrt{\overline{n}} \neq 7 \leq 9.72$ specified above, the evolution with collapses and revivals are similar to the optimal evolution at $\sqrt{\overline{n}} = 7$ in Fig.5 , Fig.6 , but the degree of purity evolves significantly below the maximum value 1, with the corresponding concurrence evolving significantly above the minimum value 0, signifying that in these cases the atom is essentially in a mixed state. Within the range $1 < \sqrt{\overline{n}} \leq 9.2$, the evolution of the spin excitation number remains precisely the same as in the $\sqrt{\overline{n}} = 7$ evolution in Fig.5 , Fig.6, but falls below the resonance spin excitation number collapse axis (below $\frac{1}{2}$-axis) in the range $9.2 < \sqrt{\overline{n}} \leq 9.72$.

We obtain interesting dynamical features of the atomic state evolution by increasing $\sqrt{\overline{n}}$ to larger values $\sqrt{\overline{n}} > 9.72$. The reverse order evolution in which the concurrence rises towards its maximum value $\mathcal{C} = 1$, while the degree of purity falls towards its minimum value $\mathcal{D} = 0$ with increasing $\sqrt{\overline{n}}$, means that at some value $\sqrt{\overline{n}} > 9.72$, the rising concurrence and the falling degree of purity can coincide and cross-over at points $\mathcal{C} = \mathcal{D} = \frac{1}{\sqrt{2}}$ on the uniformly mixed state axis. Indeed, we find that in the resonant strong coupling $0 < f < 1$ dynamics, this cross-over of concurrence and degree of purity occurs at $\sqrt{\overline{n}} = 9.785$ in the JC model plotted in Fig.7 and at $\sqrt{\overline{n}} = 9.735$ in the aJC model plotted in Fig.8, where the respective minimum and maximum points of the concurrence (red) and degree of purity (blue) coincide on the uniformly mixed state axis. We have extended the time τ-axis to show the near stability of this interesting critical evolution, which describes the dynamics of the atom in a uniformly mixed state. As expected in a mixed state, the spin excitation number has significantly diminished, undergoing steady evolution with collapses and revivals about an axis at ≈ 0.35, significantly below the resonance spin excitation number collapse axis at 0.5 in Fig.5 , Fig.6.

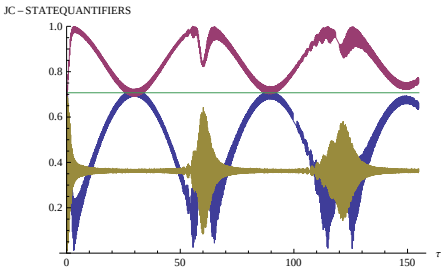

Figure 7: Resonance evolution of degree of atomic state purity $\mathcal{D}$ (BLUE), concurrence $\mathcal{C}$ (RED) and spin excitation number $\langle\sigma_+\sigma_-\rangle$ (YELLOW) in the JC model at cross-over $k = 1$; $\sqrt{\overline{n}} = 9.785$; $0 < f < 1$ over scaled time $\tau = \lambda t$

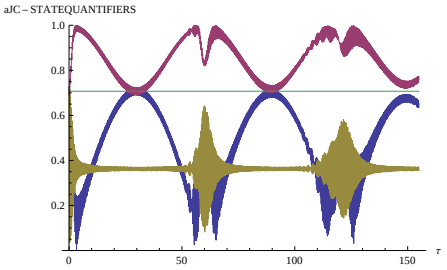

Figure 8: Resonance evolution of degree of atomic state purity $\mathcal{D}$ (BLUE), concurrence $\mathcal{C}$ (RED) and spin excitation number $\langle \sigma_- \sigma_+ \rangle$ (YELLOW) in the aJC model at cross-over $k = 1$; $\sqrt{\overline{n}} = 9.735$; $0 < f < 1$ over scaled time $\tau = \lambda t$

The interesting cross-over property of concurrence and degree of purity at large mean photon number amplitudes $\sqrt{\overline{n}} = 9.785$ in Fig.7 in the JC model and $\sqrt{\overline{n}} = 9.735$ in Fig.8 in the aJC model does not have comparison in the literature since it has never been studied in earlier works.

The concurrence continues rising as the degree of purity and spin excitation number continue falling with increasing mean photon number amplitude up to a critical value $\sqrt{\overline{n}_c} = 11.2$ where the concurrence (red) reaches its steady state time-independent maximum value $\mathcal{C} = 1$, while the degree of purity (blue-coincides with the time τ-axis) and spin excitation number (yellow-coincides with the time τ-axis) both reach their respective minimum values ($\mathcal{D} = 0$, $\langle \sigma_+ \sigma_- \rangle = 0$), which we have plotted only in the JC model in Fig.9, since the corresponding evolution at $\sqrt{\overline{n}_c} = 11.2$ in the aJC model is precisely similar. The green line is the uniformly mixed state axis. We have extended the time τ-axis to show the strictly time-independent evolution of the order parameters at $\sqrt{\overline{n}_c} = 11.2$.

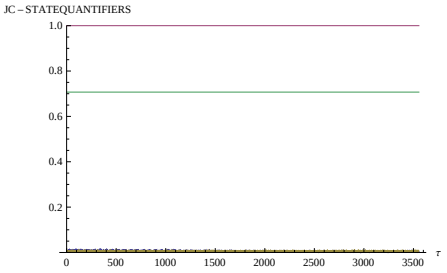

Figure 9: Resonance evolution of degree of atomic state purity $\mathcal{D}$ (BLUE-very faint at minimum value 0 along the τ-axis), concurrence $\mathcal{C}$ (RED) and spin excitation number $\langle \sigma_+ \sigma_- \rangle$ (YELLOW-very faint at minimum value 0 along the τ-axis) in the JC model at $k = 1$; $\sqrt{\overline{n}} \geq 11.2$; $0 < f < 1$ over scaled time $\tau = \lambda t$. The corresponding evolution in the aJC model is precisely similar.

The respective steady state time-independent maximum value 1 of the concurrence and minimum value 0 of the corresponding degree of purity in Fig.9 signify the evolution of the atomic state to a stable maximally entangled state at the critical mean photon number amplitude $\sqrt{\overline{n}_c} = 11.2$. This stable maximally entangled state is independent of all $\sqrt{\overline{n}} > 11.2$ and we establish below that it is completely independent of the detuning parameters $f > 0$, $k > 0$ in both JC and aJC models. It follows that in the resonant and off-resonant JC , aJC models, the mean photon number amplitude $\sqrt{\overline{n}}$ cannot be increased to arbitrarily large values, but only up to a maximum critical value $\sqrt{\overline{n}_c} = 11.2$ where the atomic state reaches a stable maximally entangled state. This qualitative maximally entangled state evolution at $\sqrt{\overline{n}} \geq 11.2$ means that the mathematical disentangling of the atomic and field mode states at large mean photon number $\overline{n} \to \infty$ in the JC model in [6 , 7] may need an alternative physical interpretation different from the pure state separability assumed therein. According to the evolution obtained within the range $1 < \sqrt{\overline{n}} < 9.72$ in resonant JC model in the present work, the pure state separability approximation in [6 , 7 , 8 , 10 , 11] may be limited to the range of values $1 < \sqrt{\overline{n}} \leq 9.3$, meaning very large mean photon numbers only up to a maximum value $\overline{n}_{max} = (9.3)^2$, noting that at $\sqrt{\overline{n}} = 9.3$, the degree of purity rises spontaneously to a short-lived maximum value $\mathcal{D}(\sqrt{\overline{n}} = 9.3) \approx 0.9$, significantly below the completely disentangled pure state maximum degree of purity $\mathcal{D} = 1$. As explained above, at values $\sqrt{\overline{n}} > 9.3$, the atomic state evolution in resonant JC model is essentially in a mixed state, such that a mathematical pure state disentanglement at $\sqrt{\overline{n}} > 9.3$ is a bad

approximation.

We observe that, in resonant strong coupling, $0 < f < 1$, JC and aJC interaction, the atomic state generally evolves asymptotically from the mixed state at $1 < \sqrt{\overline{n}} \leq 9.72$ into a stable maximally entangled state, signified by the concurrence (red) growing asymptotically to the steady state time-independent maximum value 1 and the corresponding degree of purity (blue) decaying asymptotically to the steady state time-independent minimum value 0, over a fairly long interaction time, which we have demonstrated at $\sqrt{\overline{n}} = 7$ only in the JC model in Fig.10, here again noting that the corresponding evolution at $\sqrt{\overline{n}} = 7$ in the aJC model is precisely similar. Notice that the collapse and revival evolution of the spin excitation number (yellow) remains stable, neither growing nor decaying, but develops fairly chaotic oscillations over the long interaction time.

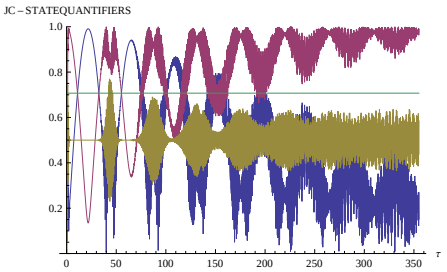

Figure 10: Resonance evolution of degree of atomic state purity $\mathcal{D}$ (BLUE), concurrence $\mathcal{C}$ (RED) and spin excitation number $\langle \sigma_+ \sigma_- \rangle$ (YELLOW) in the strong coupling JC model at $k = 1$; $\alpha = 7$; $0 < f < 1$ over scaled time $\tau = \lambda t$. The corresponding evolution in the aJC model is precisely similar.

Up to this stage, the picture which has emerged is that, except within the ground state evolution regime $0 < \sqrt{\overline{n}} = f \leq 0.1$ where the JC interaction generates only plane wave evolution of the ground state $|g0\rangle$ without spin excitations, while the aJC interaction generates blue-sideband transitions characterized by perfect Rabi oscillations between the lowest-lying qubit states $|g0\rangle$ and $|e1\rangle$, the dynamical evolution in resonant strong coupling, $0 < f < 1$, JC and aJC models takes similar form, differing only in the red-sideband transitions in the JC interaction mechanism and the blue-sideband transitions in the aJC interaction mechanism. We have established in equations (27) and (28) that the similarities are due to the approximations $f << 1$, generally $f << \sqrt{n+1}$, $n = 0, 1, 2, ...$, which effectively eliminate the residual detuning of the aJC interaction, leading to general time evolving state vectors of similar form in resonance $k = 1$ strong coupling JC and aJC models. We now proceed to the case of resonant weak coupling interaction, characterized by large residual detuning parameter $f > 1$, where the approximations in equations (27) , (28) do not apply.

3.2.2 Atomic state evolution in the resonant weak coupling interaction : $k = 1$; $f > 1$

As defined above, the weak coupling interaction is characterized by the residual detuning parameter f in the range $f > 1$, meaning $1 < f < \infty$. In the resonant weak coupling JC and aJC models, the natural evolution property of the atomic state in equation (21′) is set by

$$k = 1 \; ; \quad \epsilon = 1 \; ; \qquad \sqrt{\overline{n}} = f > 1$$

$$\text{JC} : \; R_{n+j} = \lambda \sqrt{n+j} \; ; \quad c_{n+j} = 0 \; ; \quad s_{n+j} = 1$$

$$\text{aJC} : \; \overline{R}_{n+j} = \lambda \sqrt{n+j+\overline{n}} \; ; \quad \overline{c}_{n+j} = \frac{\sqrt{\overline{n}}}{\sqrt{n+j+\overline{n}}} \; ; \quad \overline{s}_{n+j} = \frac{\sqrt{n+j}}{\sqrt{n+j+\overline{n}}} \; ; \quad j = 0, 1 \tag{29}$$

which differs from the strong coupling natural evolution property in equation (24) only in the condition that the mean photon number amplitude now takes large values $\sqrt{\overline{n}} > 1$. The procedure for determining the degree of purity, concurrence and spin excitation number in natural evolution remains the same as explained in the strong coupling case above.

We begin by recalling the well established property that, in resonance $k = 1$ dynamics, the JC interaction is completely independent of the residual detuning parameter f and is controlled only by the mean photon number amplitude $\sqrt{\overline{n}}$, which can be increased only up to the maximum value $\sqrt{\overline{n}_{max}} = 11.2$, where the atom reaches a stable maximally entangled state. This means that in resonant $k = 1$ weak coupling, $f > 1$,

interaction, the residual detuning parameter is the only free parameter which can be increased to even very large values $f >> 1$ to study the evolution of the atomic state from the uniformly mixed state in natural evolution at $\sqrt{\overline{n}} = f > 1$. Being completely independent of the detuning parameter f, the atomic state evolution in the resonant weak coupling JC model remains exactly the same as in all the cases presented in the strong coupling $0 < f < 1$ interaction in Fig.5-Fig.10 where the $\sqrt{\overline{n}}$ values are within the natural evolution range $\sqrt{\overline{n}} = f > 1$ in the weak coupling interaction. It follows that, in resonant $k = 1$ weak coupling interaction, increasing the detuning parameter f to larger values affects only aJC dynamics, where the atomic state evolution from the uniformly mixed state develops interesting physical features. Hence, for all the possible $\sqrt{\overline{n}}$ values in the weak coupling natural evolution range $1 < \sqrt{\overline{n}} = f < 11.2$, it is sufficient to present only the resonant aJC results explicitly, but note the corresponding resonant weak JC results similar to the results obtained earlier in Fig.5-Fig.10 in the resonant strong coupling interaction.

We have plotted natural evolution of the degree of purity $\overline{\mathcal{D}}$, concurrence $\overline{\mathcal{C}}$ and spin excitation number $\langle \sigma_- \sigma_+ >$ determined at $1 < \sqrt{\overline{n}} = f < 11.2$ in resonant weak coupling aJC model. We have established that natural evolution in the resonant weak coupling aJC model is composed of four distinct dynamical regimes: *reversible mixed state evolution* regime in the parameter range $1 < \sqrt{\overline{n}} = f \leq 9.2$, *irreversible mixed state evolution* regime in the parameter range $9.2 < \sqrt{\overline{n}} = f < 9.57$, *reversible entangled state evolution* regime in the parameter range $9.57 \leq \sqrt{\overline{n}} = f < 9.755$ and an *irreversible entangled state evolution* regime in the parameter range $9.755 \leq \sqrt{\overline{n}} = f < 11.2$. The maximally entangled state evolution regime, completely independent of the detuning parameters $f > 0$, $k > 0$, occurs at $\sqrt{\overline{n}} \leq 11.2$.

A. Mixed state evolution regime : $1 < \sqrt{\overline{n}} = f < 9.57$

In general, natural evolution identified as a mixed state evolution regime within the parameter range $1 < \sqrt{\overline{n}} = f < 9.57$ is composed of stable symmetrical, very nearly periodic, collapses and revivals of slowly decaying degree of purity $\overline{\mathcal{D}}$ (blue) and spin excitation number (yellow), *above* or about, and slowly growing concurrence (red), *below* or about, the uniformly mixed state axis, with the degree of purity, concurrence and spin excitation number oscillation cluster revival turning points, all coinciding exactly on the axis at points where $\overline{\mathcal{D}} = \langle \sigma_- \sigma_+ \rangle = \overline{\mathcal{C}} = \frac{1}{\sqrt{2}}$, as shown in the examples at $\sqrt{\overline{n}} = f = 7$ in Fig.11, at $\sqrt{\overline{n}} = f = 9.2$ in Fig.12 and at $\sqrt{\overline{n}} = f = 9.4$ in Fig.13, in the resonant weak coupling aJC model. Note that the corresponding natural evolution at $\sqrt{\overline{n}} = f = 7$, 9.2 , 9.4 in the resonant weak coupling JC model, completely independent of f, are precisely similar to the evolution in Fig.5 or Fig.10, determined only by $\sqrt{\overline{n}} = 7$, 9.2 , 9.4.

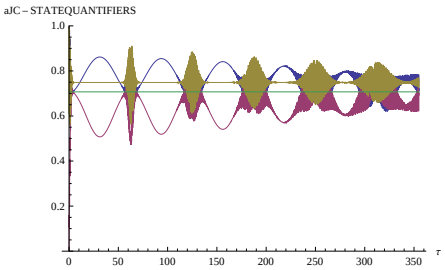

Figure 11: Natural evolution of the degree of purity $\overline{\mathcal{D}}$ (BLUE), concurrence $\overline{\mathcal{C}}$ (RED) and spin excitation number $\langle \sigma_- \sigma_+ \rangle$ (YELLOW) in resonant weak coupling aJC model at $k = 1$; $\sqrt{\overline{n}} = f = 7$ over scaled time $\tau = \lambda t$

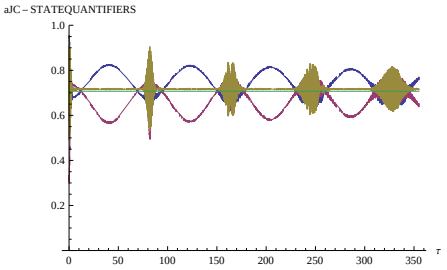

Figure 12: Natural evolution of the degree of purity $\overline{\mathcal{D}}$ (BLUE), concurrence $\overline{\mathcal{C}}$ (RED) and spin excitation number $\langle \sigma_- \sigma_+ \rangle$ (YELLOW) in resonant weak coupling aJC model at $k = 1$; $\sqrt{\overline{n}} = f = 9.2$ over scaled time $\tau = \lambda t$

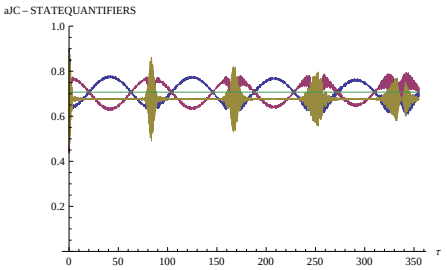

Figure 13: Natural evolution of the degree of purity $\overline{\mathcal{D}}$ (BLUE), concurrence $\overline{\mathcal{C}}$ (RED) and spin excitation number $\langle \sigma_- \sigma_+ \rangle$ (YELLOW) in resonant weak coupling aJC model at $k = 1$; $\sqrt{\overline{n}} = f = 9.4$ over scaled time $\tau = \lambda t$

In Fig.11 at $\sqrt{\overline{n}} = f = 7$ and Fig.12 at $\sqrt{\overline{n}} = f = 9.2$, the gentle rise of the asymptotically decaying degree of purity (blue) to a fairly broad maximum value above the uniformly mixed state axis, but significantly lower than the disentangled pure state maximum value 1, and the corresponding gentle fall of the asymptotically growing concurrence (red) to a minimum value below the axis, but significantly higher than the disentangled pure state minimum value 0, signifies the property that in the resonant weak coupling aJC model, the natural evolution of the atomic state is a fairly stable uniformly mixed state. In Fig.13 at $\sqrt{\overline{n}} = 9.4$, the fairly stable uniformly mixed state evolution is signified by symmetrical, essentially stable periodic oscillations of the degree of purity (blue) and the concurrence (red) about the uniformly mixed state axis (green) where the oscillations cross. Natural evolution in the mixed state regime is composed of a *reversible mixed state* regime defined within the parameter range $1 < \sqrt{\overline{n}} = f \leq 8.55$ and an *irreversible mixed state* regime defined within the parameter range $8.55 < \sqrt{\overline{n}} = f < 9.57$.

AI. Reversible mixed state evolution regime : $1 < \sqrt{\overline{n}} = f \leq 8.55$

A reversible mixed state evolution regime, determined by the parameter range $1 < \sqrt{\overline{n}} = f \leq 8.55$, is characterized by the property that the atomic state can *evolve spontaneously* from the uniformly mixed state in natural evolution at $\sqrt{\overline{n}} = f$ into a *very nearly* disentangled pure state in the JC model, and in resonant strong coupling $0 < f < 1$ aJC model, such as in Fig.5 , Fig.6, while, strictly in resonant weak coupling $f > 1$ aJC model, a reversible mixed state evolution regime $1 < \sqrt{\overline{n}} = f \leq 8.55$ is characterized by the property that the atomic state does not evolve spontaneously, but can be *driven* from the uniformly mixed state in natural evolution at $\sqrt{\overline{n}} = f$ into a *steady state completely* disentangled pure state by increasing the residual detuning parameter f up to some larger critical value $f_c = \epsilon_c \sqrt{\overline{n}} >> 1$, $\epsilon_c >> 1$.

The example of natural evolution at $\sqrt{\overline{n}} = f = 7$, plotted in Fig.11, is within the reversible mixed state evolution regime $1 < \sqrt{\overline{n}} = f \leq 8.55$. The revival oscillation clusters of the spin excitation number and the revival turning points of the degree of purity and concurrence all coincide on the uniformly mixed state axis at points where $\overline{\mathcal{D}} = \overline{\mathcal{C}} = \langle \sigma_- \sigma_+ \rangle = \frac{1}{\sqrt{2}}$.

We now consider the important characteristic property that within the reversible mixed state evolution regime, $1 < \sqrt{\overline{n}} = f \leq 8.55$ in the resonant weak coupling aJC model, the atomic state can be driven from the uniformly mixed state in natural evolution at $1 < \sqrt{\overline{n}} = f \leq 8.55$ to a steady state completely

disentangled pure state by keeping the mean photon number amplitude $\sqrt{\overline{n}}$ at the natural evolution value, but increasing the residual detuning parameter f to large critical values f_c where the degree of purity reaches the steady state time-independent maximum value $\overline{\mathcal{D}} = 1$, and the corresponding concurrence reaches the steady state time-independent minimum value $\overline{\mathcal{C}} = 0$. Increasing f to larger values progressively raises both degree of purity and spin excitation number towards the steady state time-independent maximum value 1, but progressively lowers the concurrence towards the steady state time-independent minimum value 0. Note that in studying the dynamics beyond natural evolution, the mean photon number amplitude $\sqrt{\overline{n}}$ is kept fixed at its natural evolution value, while increasing the residual detuning parameter using the general parameter unification relation $f = \epsilon\sqrt{\overline{n}}$ in equation (19) for $\sqrt{\overline{n}} > 1$, $\epsilon > 1$.

In the example of natural evolution at $\sqrt{\overline{n}} = f = 7$ in Fig.11, increasing the residual detuning parameter f to larger values $f > 7$ drives the coincident degree of purity (blue) and spin excitation number (yellow) to their steady state time-independent maximum values $\overline{\mathcal{D}} = \langle \sigma_- \sigma_+ \rangle = 1$ and the corresponding concurrence (red) to its steady state time-independent minimum value $\overline{\mathcal{C}} = 0$, at a critical value $f_c = \epsilon_c \times 7 = 100 \times 7$, i.e., $\epsilon_c = 100$, as shown in Fig.14, where the blue and yellow of the degree of purity and spin excitation number coincide on the maximum value 1-axis at the top, while the red of the concurrence at minimum value 0 coincides with the time τ-axis. The steady state time-independent maximum and minimum values of the degree of purity and concurrence ($\overline{\mathcal{D}} = 1$, $\overline{\mathcal{C}} = 0$) in Fig.14 signify the property that, on increasing the residual detuning parameter to a critical value $f_c = 100 \times 7$, the atomic state evolves from a uniformly mixed state at $\sqrt{\overline{n}} = f = 7$ to a completely disentangled pure state at $\sqrt{\overline{n}} = 7$, $f \geq 100 \times 7$.

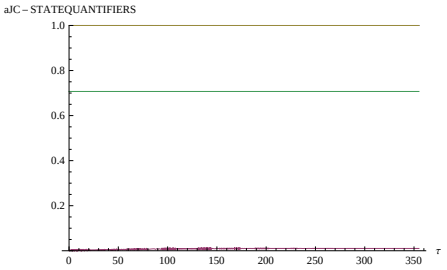

Figure 14: Evolution of the degree of purity $\overline{\mathcal{D}}$, coinciding with the spin excitation number $\langle \sigma_- \sigma_+ \rangle$ (BLUE+YELLOW) at maximum value 1 and the concurrence $\overline{\mathcal{C}}$ (RED) at minimum value 0, coinciding with the time τ-axis, at $k = 1$; $\sqrt{\overline{n}} = 7$; $f \geq 100 \times 7$ in resonant weak coupling aJC model over scaled time $\tau = \lambda t$

Hence, using the example of natural evolution at $\sqrt{\overline{n}} = 7$ in (Fig.11 , Fig.14), we have established the characteristic property that within the reversible mixed state regime $1 < \sqrt{\overline{n}} = f \leq 8.55$ in resonant weak coupling aJC dynamics, the atomic state can be driven from the uniformly mixed state into a completely disentangled pure state by increasing the residual detuning parameter to larger critical values $f_c = \epsilon_c\sqrt{\overline{n}}$, $\sqrt{\overline{n}} > 1$, $\epsilon_c^2 >> 1$.

To determine the form of the completely disentangled pure state arising within the reversible mixed state regime $1 < \sqrt{\overline{n}} = f \leq 8.55$ in the resonant weak coupling aJC dynamics at very large residual detuning parameter $f >> 1$ ($\epsilon >> 1$), we assume that for mean photon number amplitude in the range $1 < \sqrt{\overline{n}} \leq 8.55$, the field mode excitation number n in the qubits $|gn\rangle$ included in the superposition of the atom-field initial state $|\psi_{g\alpha}\rangle$ in equation (4) and the general time evolving state vectors in equations (5) , (6), is very small compared to $f^2 \to \infty$. Hence, the atomic state evolution at very large values $f >> 1$ in the resonant weak coupling aJC dynamics is determined by applying the approximation $f >> \sqrt{n+j}$, $j = 0, 1$ in the Rabi frequency and related parameters $\overline{R}_{n+j}$, $\overline{c}_{n+j}$, $\overline{s}_{n+j}$ in equation (10), which, substituted into the time evolving state vector $|\Psi_{aJC}(t)$ in equation (6), yields a completely disentangled pure state vector in the form

$$k = 1 \; ; \quad 1 < \alpha = \sqrt{\overline{n}} \leq 8.55 \; ; \quad \epsilon_c \geq 55 \; ; \quad f = f_c = \epsilon_c\sqrt{\overline{n}} >> \sqrt{n+j} \; ; \quad j = 0, 1$$

$$\epsilon >> 1 \; ; \qquad \overline{R}_{n+j} = \lambda\sqrt{n + j + \epsilon^2\overline{n}} \approx \lambda\epsilon\sqrt{\overline{n}} \; ; \qquad \overline{c}_{n+j} \approx 1 \; ; \qquad \overline{s}_{n+j} \approx 0$$

$$|\Psi_{aJC}(t)\rangle \approx e^{i\lambda\epsilon\sqrt{\overline{n}}t}|g\rangle \sum_{n=0}^{\infty} \sqrt{P_n} \; e^{-i\omega(n+1)t}|n\rangle \tag{30}$$

where $\epsilon_c = 55$ is the minimum critical value for driving natural evolution at $\sqrt{\overline{n}} = f = 8.55$ to steady state time-independent evolution at $\sqrt{\overline{n}} = 8.55$, $f = 55 \times 8.55$.

The large residual detuning parameter approximation $f >> \sqrt{n+j}$, $j = 0, 1$, in equation (30) reveals that the general time evolving state vector $|\Psi_{aJC}(t)\rangle$ which describes the steady state time-independent evolution in Fig.14 at $\sqrt{\overline{n}} = 7$, $f \geq 100 \times 7$, after driving the dynamics from the reversible mixed state evolution regime $1 < \sqrt{\overline{n}} = f \leq 8.55$ by increasing $f = \epsilon\sqrt{\overline{n}}$ in resonant weak coupling aJC model, is a completely disentangled pure state obtained as a separable product of a free time evolving atomic ground state $e^{i\lambda\epsilon\sqrt{\overline{n}}\ t}|g\rangle$ and a plane wave field mode coherent state $\sum_{n=0}^{\infty}\sqrt{P_n}\ e^{-i\omega nt}|n\rangle$, where $\sqrt{P_n}$ is defined according to equation (7). It is easy to establish that in the completely disentangled pure state $|\Psi_{aJC}(t)\rangle$ in equation (30), the degree of purity, spin excitation number and concurrence are at their respective steady state time-independent maximum and minimum values $\overline{\mathcal{D}} = \langle\sigma_-\sigma_+\rangle = 1$, $\overline{\mathcal{C}} = 0$, in agreement with the exact pure state evolution in Fig.14.

We emphasize that the evolution in the Fig.14 at $\sqrt{\overline{n}} = 7$, $f \geq 100 \times 7$ example signifies a steady state time-independent dynamics described by the completely disentangled pure state $|\Psi_{aJC}(t)\rangle$, where the atom and field mode revert to their initial ground and coherent states, each picking up global time evolving factors. This steady state time-independent evolution at large residual detuning parameter $f >> 1$ is achievable only in the resonant weak coupling aJC model, but cannot be reached in the resonant JC model, which is completely independent of f. Within the same range of values $1 < \sqrt{\overline{n}} \leq 8.55$, the resonant JC dynamics is restricted to the spontaneous evolution to a short-lived very nearly pure state in the Fig.5 at $\sqrt{\overline{n}} = 7$ example, which is described by the general time evolving resonant JC state vector $|\Psi_{JC}(t)\rangle$ in equation (28).

For completeness and ease of comparison of the completely disentangled pure state arising at $1 < \sqrt{\overline{n}} \leq 8.55$, $f >> 1$ in the resonant weak coupling aJC model and the approximations assuming very large mean photon number amplitude $\sqrt{\overline{n}} \to \infty$, in resonant JC model in [6 , 7 , 8 , 10 , 11], we generalize the initial atomic state to a superposition of the ground and excited states $\eta|e\rangle + \xi|g\rangle$, so that the atom-field mode initial state $|\psi_{g\alpha}\rangle$ in equation (4) generalizes to the form

$$|\psi_{eg\alpha}\rangle = \sum_{n=0}^{\infty}\frac{e^{-\frac{1}{2}\alpha^2}\alpha^n}{\sqrt{n!}}(\eta|e\rangle + \xi|gn\rangle)\ ; \qquad |\eta|^2 + |\xi|^2 = 1 \tag{31}$$

The respective general time evolving state vectors $|\Psi_{JC}(t)\rangle$, $|\Psi_{aJC}(t)\rangle$ generated by the JC and aJC Hamiltonians H_{JC} , H_{aJC} in equation (3) are obtained in the form [2 , 14]

$$\text{JC} \ : \quad |\Psi_{JC}(t)\rangle = \eta|\Psi_{JC}^{e\alpha}(t)\rangle + \xi|\Psi_{JC}^{g\alpha}(t)\rangle$$

$$|\Psi_{JC}^{e\alpha}(t)\rangle = \sum_{n=0}^{\infty}(\ \sqrt{P_n}e^{-i\omega(n+\frac{1}{2})t}(\cos(R_{en+1}t) - ic_{en+1}\sin(R_{en+1}t))|e\rangle - i\ \sqrt{P_{n-1}}e^{-i\omega(n-\frac{1}{2})t}s_{en}\sin(R_{en}t)|g\rangle\ )|n\rangle$$

$$|\Psi_{JC}^{g\alpha}(t)\rangle = \sum_{n=0}^{\infty}(\ \sqrt{P_n}e^{-i\omega(n-\frac{1}{2})t}(\cos(R_{gn}t) + ic_{gn}\sin(R_{gn}t))|g\rangle - i\ \sqrt{P_{n+1}}e^{-i\omega(n+\frac{1}{2})t}s_{gn+1}\sin(R_{gn+1}t)|e\rangle\ )|n\rangle \tag{32}$$

$$\text{aJC} \ : \quad |\Psi_{aJC}(t)\rangle = \eta|\Psi_{aJC}^{e\alpha}(t)\rangle + \xi|\Psi_{aJC}^{g\alpha}(t)\rangle$$

$$|\Psi_{aJC}^{e\alpha}(t)\rangle = \sum_{n=0}^{\infty}(\ \sqrt{P_n}e^{-i\omega(n+\frac{1}{2})t}(\cos(\overline{R}_{en}t) - i\overline{c}_{en}\sin(\overline{R}_{en}t))|e\rangle - i\ \sqrt{P_{n+1}}e^{-i\omega(n+\frac{3}{2})t}\overline{s}_{en+1}\sin(\overline{R}_{en+1}t)|g\rangle\ )|n\rangle$$

$$|\Psi_{aJC}^{g\alpha}(t)\rangle = \sum_{n=0}^{\infty}(\ \sqrt{P_n}e^{-i\omega(n+\frac{3}{2})t}(\cos(\overline{R}_{gn+1}t) + i\overline{c}_{gn+1}\sin(\overline{R}_{gn+1}t))|g\rangle - i\ \sqrt{P_{n-1}}e^{-i\omega(n+\frac{1}{2})t}\overline{s}_{gn}\sin(\overline{R}_{gn}t)|e\rangle\ )|n\rangle \tag{33}$$

where, in equations (32) , (33), the Rabi frequencies and related parameters (R, c, s) , $(\overline{R}, \overline{c}, \overline{s})$, with indices $en+j$, $gn+j$, $j = 0, 1$, now specified by excited and ground state symbols e , g, are defined as in equations (5) , (6) , (10) as appropriate.

As usual, under resonance $k = 1$, the JC general time evolving state vector $|\Psi_{JC}(t)\rangle$ in equation (32) is completely independent of the residual detuning parameter f, thus not affected by the $f >> 1$ approximation in equation (30). On the other hand, the aJC general time evolving state vector $|\Psi_{aJC}(t)\rangle$ in equation (33) is intrinsically dependent on the residual detuning parameter f, and for resonance $k = 1$ evolution at mean photon number amplitude in the range $1 < \sqrt{\overline{n}} \leq 8.55$, applying the $f >> 1$ approximation in equation (30) to equation (33) yields the expected completely disentangled pure state in the form

$$1 < \sqrt{\overline{n}} \leq 8.55\ ; \quad f = f_c = \epsilon_c\sqrt{\overline{n}}\ ; \quad \epsilon_c \geq 55$$

$$\epsilon >> 1 \ : \quad |\Psi_{aJC}(t)\rangle \approx \Big(\eta e^{-i\frac{1}{2}\omega t}e^{-i\lambda\epsilon\sqrt{\overline{n}}t}|e\rangle + \xi e^{-i\frac{3}{2}\omega t}e^{i\lambda\epsilon\sqrt{\overline{n}}t}|g\rangle\Big)\sum_{n=0}^{\infty}\sqrt{P_n}\ e^{-i\omega nt}|n\rangle \tag{34}$$

Here again, the large $f = \epsilon\sqrt{\overline{n}} >> \sqrt{n+j}$, $j = 0, 1$, approximate state vector $|\Psi_{aJC}(t)\rangle$ in equation (34) reveals the physical property that, in the steady state time-independent evolution in resonant weak coupling aJC model, the atom and field mode both revert to their respective initial coherent states after picking up time evolving phase factors.

We observe that, the physical property of a completely disentangled pure state describing steady state time-independent evolution in resonant weak coupling aJC model is entirely different from the physical interpretation of the spontaneous evolution to a short-lived very nearly pure state in the corresponding resonant JC model given in [7 , 8 , 10]. Specifically, in [7 , 8] and related studies thereafter, it is assumed that in the very large $\overline{n} \to \infty$ limit, the general time evolving JC state vector $|\Psi_{JC}(t)\rangle$ in equation (28), which describes the evolution in Fig.5 at $\sqrt{\overline{n}} = 7$ in the resonant JC model, can be reduced to an approximately disentangled pure state composed of coherent atomic and field mode states similar to the form in equation (34). It is evident in Fig.7 at $\sqrt{\overline{n}} = 9.785$ and Fig.9 at $\sqrt{\overline{n}} \geq 11.2$ where the atomic state evolution is already in the entangled state regime in the resonant JC model, that the $\overline{n} \to \infty$ approximation in [7 , 8] needs a redefinition of the physical interpretation of the pure state disentanglement.

In an interesting related study of atomic state coherence in resonant JC model in [11], Goldberg and Steinberg imposed a recursion relation to derive a disentangled pure state expressed as a separable product of atomic and field mode coherent states, thereby interpreting the field mode state as a transcoherent state. The recursion relation in [11] is easily achieved by setting equal the coefficients of the atomic ground and excited state vectors $|g\rangle$, $|e\rangle$ in $|\Psi_{JC}(t)\rangle$, $|\Psi_{aJC}(t)\rangle$ in equation (28), giving (ignoring normalization factors)

JC

$$\sqrt{P_n}e^{i\omega t}\cos(\lambda\sqrt{n}t) = -i\ \sqrt{P_{n+1}}\sin(\lambda\sqrt{n+1}t)\ ; \quad |\Psi_{JC}(t)\rangle \to (|g\rangle + |e\rangle)\sum_{n=0}^{\infty}\sqrt{P_n}e^{-i\omega nt}\cos(\lambda\sqrt{n}t)|n\rangle$$

aJC

$$\sqrt{P_n}e^{-i\omega t}\cos(\lambda\sqrt{n+1}t) = -i\ \sqrt{P_{n-1}}\sin(\lambda\sqrt{n}t)\ ; \quad |\Psi_{aJC}(t)\rangle \to (|g\rangle + |e\rangle)\sum_{n=0}^{\infty}\sqrt{P_n}e^{-i\omega nt}\cos(\lambda\sqrt{n+1}t)|n\rangle \tag{35}$$

We observe that the recursion relation imposed in [11], and obtained here in equation (35), does not follow from any physical conditions, but is applied as a purely mathematically effective condition for generating a disentangled pure state with a coherent atomic state. In [11], the authors have elaborated how the recursion relation can be used to determine experimentally realizable forms of the JC disentangled pure state in equation (35). In the present study, we have not considered a physical condition for disentangling $|\Psi_{JC}(t)\rangle$ in equation (28) in the separable pure state form in equation (35).

AII. Irreversible mixed state evolution regime : $8.55 < \sqrt{\overline{n}} = f < 9.57$

An irreversible mixed state evolution regime, determined by the fairly narrow parameter range $8.55 < \sqrt{\overline{n}} = f < 9.57$, is characterized by the property that the atomic state *cannot* evolve spontaneously and *cannot be driven*, from the uniformly mixed state in natural evolution at $f = \sqrt{\overline{n}}$ into a very nearly or completely, disentangled pure state, but remains in a mixed state even on increasing the residual detuning parameter f to very very large values $f \to \infty$. In this regime, for all large $f \to \infty$, the time-independent maximum value of the coinciding degree of purity and spin excitation number remain above the uniformly mixed state axis, but significantly below the completely disentangled pure state value 1 in the range $\frac{1}{\sqrt{2}} < \overline{\mathcal{D}} = \langle\sigma_-\sigma_+\rangle < 0.98$, while the corresponding time-independent minimum value of the concurrence remains below the uniformly mixed state axis, but significantly above the completely disentangled pure state value 0 in the range $0.05 < \overline{\mathcal{C}} < \frac{1}{\sqrt{2}}$, signifying that the atom is generally in a mixed state.

The examples of natural evolution at $\sqrt{\overline{n}} = f = 9.2$, 9.4, plotted in Fig.12 , Fig.13, respectively, are within the irreversible mixed state evolution regime $8.55 < \sqrt{\overline{n}} = f < 9.57$, in the resonant weak coupling aJC model, noting that the corresponding evolution at $\sqrt{\overline{n}} = f = 9.2$, 9.4 in the resonant weak coupling JC model is similar to the evolution in Fig.5 at $\sqrt{\overline{n}} = 7$ or Fig.10 over long interaction time, in resonant strong coupling $0 < f < 1$ JC model.

We note that, for parameter values up to $\sqrt{\overline{n}} = f = 9$, natural evolution within the irreversible mixed state regime $8.55 < \sqrt{\overline{n}} = f < 9.57$ takes precisely the form of natural evolution at $\sqrt{\overline{n}} = f = 7$ in Fig.11, and then, in the range of parameter values $9 < \sqrt{\overline{n}} = f < 9.57$, the natural evolution advances into essentially periodic oscillations of the degree of purity and concurrence about or very nearly on, the uniformly mixed state axis, as in the examples at $\sqrt{\overline{n}} = f = 9.2$ in Fig.12 and at $\sqrt{\overline{n}} = f = 9.4$ in Fig.13. Notice that at $\sqrt{\overline{n}} = f = 9.2$, Fig.12 reveals a spectacular dynamical feature that, the collapse-axis (yellow) of the spin excitation number coincides with the uniformly mixed state axis (green). This is an interesting phenomenon in natural evolution within the range of parameter values $9 < \sqrt{\overline{n}} = f < 9.57$, defining dynamics at the boundary of the irreversible mixed state evolution regime and the entangled state regime $9.57 \leq \sqrt{\overline{n}} = f < 11.2$ described below.

In natural evolution at $\sqrt{\overline{n}} = f = 9.2$ in Fig.12, keeping the mean photon number amplitude at the natural evolution value $\sqrt{\overline{n}} = 9.2$, but increasing the residual detuning parameter to larger values $f > 9.2$ drives the coincident degree of purity (blue) and spin excitation number (yellow) to their steady state time-independent maximum values $\overline{\mathcal{D}} = \langle \sigma_- \sigma_+ \rangle = 0.95$, significantly lower than the disentangled pure state value 1, and the corresponding concurrence (red), to its steady state time-independent minimum value $\overline{\mathcal{C}} = 0.3$, significantly higher than the disentangled pure state value 0, at a critical value $f_c = 18 \times 9.2$ (meaning $\epsilon_c = 18$), as shown in Fig.15, signifying the atomic state evolution from a uniformly mixed state at $\sqrt{\overline{n}} = f = 9.2$ to a stable mixed state describing steady state time-independent evolution at $\sqrt{\overline{n}} = 9.2$, $f \geq 18 \times 9.2$.

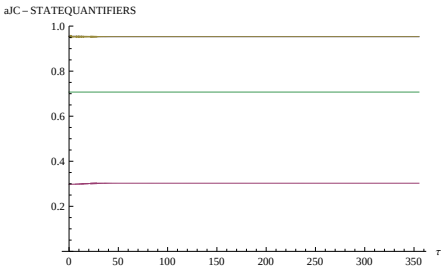

Figure 15: Evolution of the degree of purity $\overline{\mathcal{D}}$, coinciding with the spin excitation number $\langle \sigma_- \sigma_+ \rangle$ (BLUE+YELLOW), at maximum value 0.95 and the concurrence $\overline{\mathcal{C}}$ (RED) at minimum value 0.3, at $k = 1$; $\sqrt{\overline{n}} = 9.2$; $f \geq 18 \times 9.2$ in resonant weak coupling aJC model over scaled time $\tau = \lambda t$

Similarly, in natural evolution at $\sqrt{\overline{n}} = f = 9.4$, keeping $\sqrt{\overline{n}} = 9.4$, but increasing the residual detuning parameter to larger values $f > 9.4$ drives the coincident degree of purity (blue) and spin excitation number (yellow) to their steady state time-independent maximum values $\overline{\mathcal{D}} = \langle \sigma_- \sigma_+ \rangle = 0.9$, significantly lower than the disentangled pure state value 1, and the corresponding concurrence (red) to its steady state time-independent minimum value $\overline{\mathcal{C}} \approx 0.44$, significantly higher than the disentangled pure state value 0, at a critical value $f_c = 12 \times 9.4$, signifying the atomic state evolution from a uniformly mixed state at $\sqrt{\overline{n}} = f = 9.4$ to a stable mixed state describing steady state time-independent evolution at $\sqrt{\overline{n}} = 9.4$, $f \geq 12 \times 9.4$. The mixed state evolution at $\sqrt{\overline{n}} = 9.4$, $f \geq 12 \times 9.4$ is similar to the mixed state evolution at $\sqrt{\overline{n}} = 9.2$, $f \geq 18 \times 9.2$ in Fig.15, thus not very necessary to present.

The examples of natural evolution at $\sqrt{\overline{n}} = f = 9.2$, 9.4 in Fig.12 , Fig.13, developing into general stable mixed state evolution on increasing the residual detuning parameter to very large values $f \geq 18 \times 9.2$, 12×9.4, respectively, taking similar form as in Fig.15, signify that, within the irreversible mixed state regime $8.55 < \sqrt{\overline{n}} = f < 9.57$, the atomic state cannot evolve spontaneously, and cannot be driven, to a disentangled pure state, but remains a mixed state. This is the characteristic dynamical feature of the irreversible mixed state evolution regime.

Increasing the natural evolution parameter $\sqrt{\overline{n}} = f$ to larger values $\sqrt{\overline{n}} = f \geq 9.57$ drives the atomic state evolution into a regime where the concurrence is generally higher than the degree of purity, which we identify as an entangled state regime, defined within the parameter range $9.57 \leq \sqrt{\overline{n}} = f < 11.2$, which we now describe.

B. Entangled state evolution regime : $9.57 \leq \sqrt{\overline{n}} = f < 11.2$

Natural evolution identified as an entangled state evolution regime within the parameter range $9.57 \leq \sqrt{\overline{n}} = f < 11.2$ is composed of a higher fairly stable concurrence evolving periodically on or *above* the uniformly

mixed state axis and lower fairly stable degree of purity and spin excitation number evolving periodically on or *below* the uniformly mixed state axis, as shown in the examples at $\sqrt{\overline{n}} = f = 9.57$ in Fig.16 and $\sqrt{\overline{n}} = f = 9.735$ in Fig.17 in the resonant weak coupling aJC model. Notice that natural evolution at $\sqrt{\overline{n}} = f = 9.57$ in Fig.16 is essentially similar to the evolution in Fig.7 at $\sqrt{\overline{n}} = 9.785$ and Fig.8 at $\sqrt{\overline{n}} = 9.735$ in resonant strong coupling $(0 < f < 1)$ JC and aJC models.

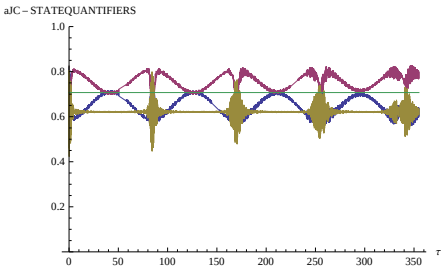

Figure 16: Natural evolution of the degree of purity $\overline{\mathcal{D}}$ (BLUE), concurrence $\overline{\mathcal{C}}$ (RED) and spin excitation number $\langle \sigma_- \sigma_+ \rangle$ (YELLOW) in resonant weak coupling aJC model at $k = 1$; $\sqrt{\overline{n}} = f = 9.57$ over scaled time $\tau = \lambda t$

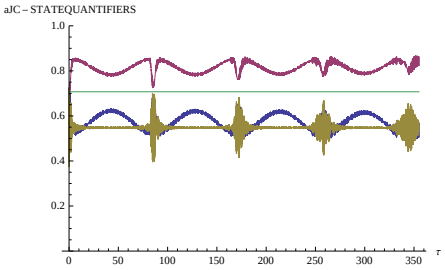

Figure 17: Natural evolution of the degree of purity $\overline{\mathcal{D}}$ (BLUE), concurrence $\overline{\mathcal{C}}$ (RED) and spin excitation number $\langle \sigma_- \sigma_+ \rangle$ (YELLOW) in resonant weak coupling aJC model at $k = 1$; $\sqrt{\overline{n}} = f = 9.735$ over scaled time $\tau = \lambda t$

Natural evolution in the entangled state regime is composed of a *reversible entangled state* regime defined within the parameter range $9.57 \leq \sqrt{\overline{n}} = f < 9.755$ and an *irreversible entangled state* regime defined within the parameter range $9.755 \leq \sqrt{\overline{n}} = f < 11.2$.

BI. Reversible entangled state evolution regime : $9.57 \leq \sqrt{\overline{n}} = f < 9.755$

A reversible entangled state evolution regime is described by natural evolution at $\sqrt{\overline{n}} = f$ within the parameter range $9.57 \leq \sqrt{\overline{n}} = f < 9.755$. The defining dynamical property of the reversible entangled state evolution regime is that increasing the residual detuning parameter f to larger values lowers the concurrence from above to below, while raising the coinciding degree of purity and spin excitation number from below to above, the uniformly mixed state axis, thus driving the atomic state to a stable mixed state. Keeping $\sqrt{\overline{n}}$ at the natural evolution value, but increasing f reveals that the reversible entangled state evolution regime is characterized by two important dynamical properties (i) the degree of purity, concurrence and spin excitation number all coincide and evolve periodically on the uniformly mixed state axis (ii) the atomic state cannot develop spontaneously or be driven, into a nearly or completely disentangled pure state, but can only reach an irreversible mixed state signified by coinciding degree of purity and spin excitation number steady state time-independent maximum value $\frac{1}{\sqrt{2}} < \overline{\mathcal{D}} = \langle \sigma_- \sigma_+ \rangle \leq 0.82$, above the uniformly mixed state axis, and concurrence steady state time-independent minimum value $0.57 \leq \overline{\mathcal{C}} < \frac{1}{\sqrt{2}}$, below the uniformly mixed state axis. The examples of natural evolution at $\sqrt{\overline{n}} = f = 9.57$ in Fig.16 and $\sqrt{\overline{n}} = f = 9.735$ in Fig.17 are within the reversible entangled state evolution regime $9.57 \leq \sqrt{\overline{n}} = f < 9.755$.

In the natural evolution at $\sqrt{\overline{n}} = f = 9.57$ in Fig.16 and at $\sqrt{\overline{n}} = f = 9.735$ in Fig.17, keeping the mean photon number amplitude at the respective natural evolution values $\sqrt{\overline{n}} = 9.57$, 9.735, but increasing the residual detuning parameter $f = \epsilon\sqrt{\overline{n}}$ to respective larger values $f > 9.57$, $f > 9.735$ $(\epsilon >> 1)$, generates

evolution characterized by the degree of purity, concurrence and spin excitation number all nearly or exactly coinciding and evolving periodically on the uniformly mixed state axis at $\sqrt{\overline{n}} = 9.57$, $f = \frac{3}{2} \times 9.57$ in Fig.18 and $\sqrt{\overline{n}} = 9.735$, $f = 4 \times 9.735$ in Fig.19, respectively.

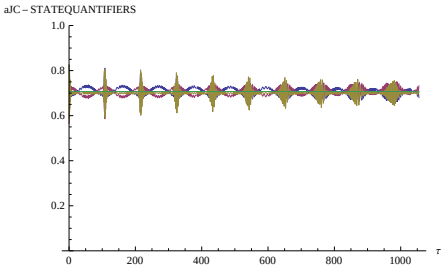

Figure 18: Natural evolution of the degree of purity $\overline{\mathcal{D}}$ (BLUE), concurrence $\overline{\mathcal{C}}$ (RED) and spin excitation number $\langle \sigma_- \sigma_+ \rangle$ (YELLOW) in resonant weak coupling aJC model at $k = 1$; $\sqrt{\overline{n}} = 9.57$, $f = \frac{3}{2} \times 9.57$ over scaled time $\tau = \lambda t$

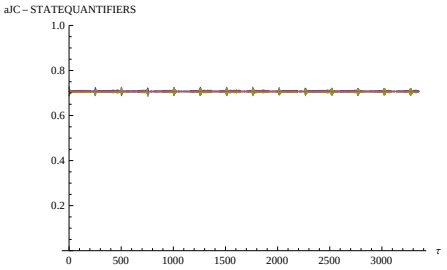

Figure 19: Natural evolution of the degree of purity $\overline{\mathcal{D}}$ (BLUE), concurrence $\overline{\mathcal{C}}$ (RED) and spin excitation number $\langle \sigma_- \sigma_+ \rangle$ (YELLOW) in resonant weak coupling aJC model at $k = 1$; $\sqrt{\overline{n}} = 9.735$, $f = 4 \times 9.735$ over scaled time $\tau = \lambda t$

Increasing f further to larger values $f \geq 18 \times 9.57$, the natural evolution at $\sqrt{\overline{n}} = f = 9.57$ in Fig.16 develops into an irreversible mixed state signified by coinciding degree of purity and spin excitation number steady state time-independent maximum value at $\overline{\mathcal{D}} = \langle \sigma_- \sigma_+ \rangle = 0.82$ and the concurrence steady state time-independent minimum value at $\overline{\mathcal{C}} = 0.57$. Similarly, increasing f further to larger values $f \geq 18 \times 9.735$, the natural evolution at $\sqrt{\overline{n}} = f = 9.735$ in Fig.17 develops into an irreversible mixed state signified by coinciding degree of purity and spin excitation number steady state time-independent maximum value at $\overline{\mathcal{D}} = \langle \sigma_- \sigma_+ \rangle \approx 0.725$ and concurrence steady state time-independent minimum value at $\overline{\mathcal{C}} \approx 0.69$. Except for their lower maximum and higher minimum values, the evolution at $\sqrt{\overline{n}} = 9.57$, $f \geq 18 \times 9.57$ and at $\sqrt{\overline{n}} = 9.735$, $f \geq 18 \times 9.735$ are both precisely similar to the corresponding irreversible mixed state evolution at $\sqrt{\overline{n}} = 9.2$, $f \geq 18 \times 9.2$ in Fig.15.

BII. Irreversible entangled state evolution regime : $9.755 \leq \sqrt{\overline{n}} = f < 11.2$

An irreversible entangled state evolution regime is described by natural evolution at $\sqrt{\overline{n}} = f$ within the parameter range $9.755 \leq \sqrt{\overline{n}} = f < 11.2$, in the general form in Fig.17, where the concurrence (red) evolves significantly above, while the coinciding degree of purity (blue) and spin excitation number (yellow) evolve below, the uniformly mixed state axis (green). The irreversible entangled state regime is characterized by two important dynamical properties (i) in the natural and driven evolution, the concurrence *cannot fall below*, and, similarly, the coinciding degree of purity and spin excitation number *cannot rise above*, the uniformly mixed state axis (ii) the atomic state cannot develop spontaneously or by driving, into a completely disentangled pure state, nor into a basic reversible or irreversible mixed state, but remains in an irreversible entangled state, where, even after increasing the residual detuning parameter f to very large values $f \to \infty$, the steady state time-independent minimum value of the concurrence remains in the higher range $\frac{1}{\sqrt{2}} \leq \overline{\mathcal{C}} < 1$, on or above, the uniformly mixed state axis and the steady state time-independent maximum value of the corresponding

coinciding degree of purity and spin excitation number remains in the lower range $0 < \overline{\mathcal{D}} = \langle \sigma_- \sigma_+ \rangle \leq \frac{1}{\sqrt{2}}$, on or below, the uniformly mixed state axis.

As examples, natural evolution at $\sqrt{\overline{n}} = f = 9.755$ and $\sqrt{\overline{n}} = f = 10$ takes the form in Fig.17 at $\sqrt{\overline{n}} = f = 9.735$, where the concurrence (red) is generally higher, evolving above, while the coinciding degree of purity (blue) and spin excitation number (yellow) are generally lower, evolving below, the uniformly mixed state axis.

In natural evolution at $\sqrt{\overline{n}} = f = 9.755$, at the boundary into the irreversible entangled state regime $9.755 \leq \sqrt{\overline{n}} = f < 11.2$, keeping $\sqrt{\overline{n}} = 9.755$, but increasing f to very large values $f \geq 18 \times 9.755$, drives the atomic state into the critical irreversible entangled state where the minimum concurrence and maximum degree of purity and spin excitation number all coincide and remain steady state time-independent at $\overline{\mathcal{C}} = \overline{\mathcal{D}} = \langle \sigma_- \sigma_+ \rangle = \frac{1}{\sqrt{2}}$ on the uniformly mixed state axis, as shown in Fig.20 at $\sqrt{\overline{n}} = 9.755$, $f \geq 18 \times 9.755$.

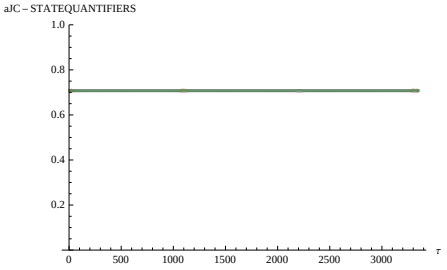

Figure 20: Evolution of the degree of purity $\overline{\mathcal{D}}$ (BLUE), concurrence $\overline{\mathcal{C}}$ (RED) and spin excitation number $\langle \sigma_- \sigma_+ \rangle$ (YELLOW) all coinciding on the uniformly mixed state axis (with equal time-independent value $\overline{\mathcal{D}} = \langle \sigma_- \sigma_+ \rangle = \overline{\mathcal{C}} = \frac{1}{\sqrt{2}}$) at $k = 1$; $\sqrt{\overline{n}} = 9.755$; $f \geq 18 \times 9.755$ in resonant weak coupling aJC model over scaled time $\tau = \lambda t$

In natural evolution at $\sqrt{\overline{n}} = f = 10$, right into the irreversible entangled state regime, keeping $\sqrt{\overline{n}} = 10$, but increasing f to very large values $f \geq 11 \times 10$, drives the atomic state into an irreversible entangled state where the steady state time-independent minimum concurrence (red) is at $\overline{\mathcal{C}} \approx 0.85$ and steady state time-independent maximum value of the coinciding degree of purity and spin excitation number is at $\overline{\mathcal{D}} = \langle \sigma_- \sigma_+ \rangle \approx 0.525$, as shown in Fig.21 at $\sqrt{\overline{n}} = 10$, $f \geq 11 \times 10$.

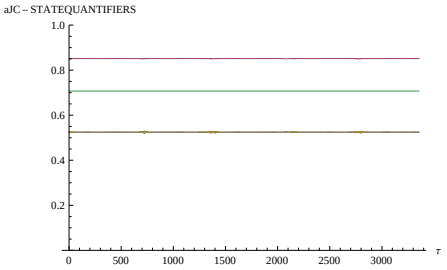

Figure 21: Evolution of the degree of purity $\overline{\mathcal{D}}$ (BLUE) coinciding with spin excitation number $\langle \sigma_- \sigma_+ \rangle$ (YELLOW) at 0.525 and concurrence $\overline{\mathcal{C}}$ (RED) at 0.85 at $k = 1$; $\sqrt{\overline{n}} = 10$; $f \geq 11 \times 10$ in resonant weak coupling aJC model over scaled time $\tau = \lambda t$

C. Maximally entangled state evolution regime : $\sqrt{\overline{n}} \geq 11.2$

Finally, we have established that, at $\sqrt{\overline{n}} \geq 11.2$, the atomic state enters a maximally entangled state for all $f > 0$. This maximally entangled state at $\sqrt{\overline{n}} \geq 11.2$ was first determined and presented in Fig.9 in the strong coupling $0 < f < 1$ interaction, but remains valid for all $f \to \infty$ in the weak coupling $f > 1$ interaction, meaning that the maximally entangled state at $\sqrt{\overline{n}} \geq 11.2$ is completely independent of the residual detuning parameter $f > 0$. It follows that in the JC and aJC models, $\sqrt{\overline{n_c}} = 11.2$ is the maximum achievable critical mean photon number amplitude at which the atomic state evolution enters a maximally entangled state completely independent of all $\sqrt{\overline{n}} > 11.2$ and residual detuning parameter $f > 0$, as in Fig.9.

In this respect, the general time evolving maximally entangled state vector in resonant JC and aJC models is obtained by setting $k = 1$, $\sqrt{\overline{n}} = 11.2$ and dropping all terms proportional to f in the Rabi frequencies and related parameters in equations (5) , (6) , (10). The maximally entangled state vectors then take the form $|\Psi_{JC}(t)\rangle$, $|\Psi_{aJC}(t)\rangle$ in equation (28) at $\sqrt{\overline{n}} = 11.2$.

Having captured the main physical features of resonance $k = 1$ dynamics in the JC and aJC models, we now generalize the description to off-resonance $k \neq 1$ in the next subsection.

3.3 Off-resonance $k \neq 1$ dynamics

According to the unified definitions of detuning parameters $\beta = (k-1)f$, $\overline{\beta} = (k+1)f$ in equation (8), off-resonance dynamics property $k \neq 1$ now means that both JC and aJC interaction mechanisms are determined by the residual detuning parameter $f > 0$. In contrast to the resonance dynamics where fixing $k = 1$ leaves the mean photon number amplitude $\sqrt{\overline{n}}$ and the residual detuning parameter f as the only variable physical parameters, off-resonance dynamics condition $k \neq 1$ now means that the atom-field mode frequency detuning parameter k also becomes a variable parameter for determining characteristic features of the atom-field interaction. This challenge of the number of variable physical parameters has been addressed by introducing the natural evolution property in which the mean photon number amplitude $\sqrt{\overline{n}}$, the residual detuning parameter f and the atom-field mode frequency detuning parameter k have been unified in simple relations in resonance $k = 1$ and off-resonance $k \neq 1$ interaction in equations (19) , (21) , (22). In resonance dynamics, the natural evolution property $f = \sqrt{\overline{n}}$ separately uses $\sqrt{\overline{n}}$ as the only variable physical parameter for defining evolution in a uniformly mixed state in specified ranges of values and then separately increasing $f = \epsilon\sqrt{\overline{n}}$, $\epsilon > 1$, to determine general features of the dynamics.

To achieve the beautiful model of dynamics, separately using only $\sqrt{\overline{n}}$ to define evolution in a uniformly mixed state in off-resonance $k \neq 1$ dynamics, we begin by applying the synchronized off-resonance natural evolution property defined in equation (22), effectively eliminating f, to express the JC and aJC Rabi frequencies R_{n+j} , $\overline{R}_{n+j}$ and the respective related interaction parameters in equation (10) in the form

$$k \neq 1 \ : \quad \sqrt{\overline{n}} = \frac{1}{2}kf \ ; \quad \Rightarrow \quad f = 2\frac{\sqrt{\overline{n}}}{k} \ ; \quad 0 < k < \infty$$

$$\text{JC} : \ R_{n+j} = \lambda\sqrt{n+j+\left(\frac{k-1}{k}\right)^2\overline{n}} \ ; \quad c_{n+j} = \frac{\left(\frac{k-1}{k}\right)\sqrt{\overline{n}}}{\sqrt{n+j+\left(\frac{k-1}{k}\right)^2\overline{n}}} \ ; \quad s_{n+j} = \frac{\sqrt{n+j}}{\sqrt{n+j+\left(\frac{k-1}{k}\right)^2\overline{n}}}$$

$$\text{aJC} : \ \overline{R}_{n+j} = \lambda\sqrt{n+j+\left(\frac{k+1}{k}\right)^2\overline{n}} \ ; \quad \overline{c}_{n+j} = \frac{\left(\frac{k+1}{k}\right)\sqrt{\overline{n}}}{\sqrt{n+j+\left(\frac{k+1}{k}\right)^2\overline{n}}} \ ; \quad \overline{s}_{n+j} = \frac{\sqrt{n+j}}{\sqrt{n+j+\left(\frac{k+1}{k}\right)^2\overline{n}}} \quad (35)$$

which shows that, in general off-resonance $k \neq 1$ dynamics, natural evolution is effectively controlled only by the mean photon number amplitude $\sqrt{\overline{n}}$ and the atom-field mode frequency detuning parameter k.

Before considering general off-resonance dynamics, we highlight two special dynamical conditions which essentially eliminate k as a variable parameter

A. Maximally entangled state evolution at $\sqrt{\overline{n}} \geq 11.2$

We have established that at $\sqrt{\overline{n}} \geq 11.2$, the evolution reaches and remains in a maximally entangled state as in Fig.9 ($0 < f < \infty$) for all $0 < k < \infty$, now leading to the general property that the maximally entangled state evolution at $\sqrt{\overline{n}} \geq 11.2$ is completely independent of both f and k

B. Large $k \to \infty$

It is easily established that at very large $k \to \infty$, (normally interpreted as thermodynamic equilibrium limit $\frac{\omega_0}{\omega} \to \infty$ [16]), the Rabi frequencies and related parameters in equation (35) reduce to the form

$$k \to \infty \ : \quad \frac{k \mp 1}{k} \approx 1 \ ; \qquad R_{n+j} \approx \lambda\sqrt{n+j+\overline{n}} \equiv \overline{R}_{n+j} \ ; \qquad c_{n+j} \approx \frac{\sqrt{\overline{n}}}{\sqrt{n+j+\overline{n}}} \equiv \overline{c}_{n+j}$$

$$s_{n+j} \approx \frac{\sqrt{n+j}}{\sqrt{n+j+\overline{n}}} \equiv \overline{s}_{n+j} \tag{36}$$

which depend on $\sqrt{\overline{n}}$, but are completely independent of k. Hence, at $k \to \infty$, the mean photon number amplitude $\sqrt{\overline{n}}$ is the only variable physical parameter which determines the natural evolution of the atomic state in off-resonant JC and aJC models. Notice that the Rabi frequencies and related interaction parameters at $k \to \infty$ in equation (36) are exactly equal to the Rabi frequency and related interaction parameters define in the natural evolution property in resonant weak coupling aJC model in equation (29), meaning that the $k \to \infty$ off-resonant JC and aJC natural evolution precisely reproduces all characteristic features of the resonant $k = 1$ aJC natural evolution in the parameter ranges $0 < \sqrt{\overline{n}} \leq 0.1$ in Fig.2, $0.1 < \sqrt{\overline{n}} < 1$ in Fig.4, $1 < \sqrt{\overline{n}} \leq 8.55$ in Fig.6 , Fig.10 , Fig.11, $8.55 < \sqrt{\overline{n}} < 9.57$ in Fig.12 , Fig.13 and $9.57 \leq \sqrt{\overline{n}} < 11.2$ in Fig.8 , Fig.16 , Fig.17, which we have confirmed already at $k = 20.755$ as an example of very large $k \to \infty$. Note that, within the ground state evolution regime $0 < \sqrt{\overline{n}} \leq 0.1$, the $k \to \infty$ off-resonant JC natural evolution reproduces precisely the resonant $k = 1$ JC natural evolution in Fig.1, as expected.

We observe that the $k \to \infty$ off-resonant JC and aJC natural evolution defined in equation (36), which precisely reproduces the resonant $k = 1$ aJC natural evolution over the parameter range $0 < \sqrt{\overline{n}} \leq 11.2$, is fixed and cannot describe the development from natural evolution into a completely disentangled pure state and into an entangled state, which we have established to be achievable on increasing the residual detuning parameter to very large values $f \to \infty$ in the resonant $k = 1$ aJC model. We now go back to the general definition of off-resonance $k \neq 1$ natural evolution in equation (35).

3.3.1 General off-resonance $k \neq 1$ natural evolution

To define off-resonance natural evolution in a general form, we maintain the property that the mean photon number amplitude remains the only variable parameter $\sqrt{\overline{n}}$. In this respect, we consider k to be proportional to $\sqrt{\overline{n}}$ in the form $k = \nu\sqrt{\overline{n}}$, where ν is a numerical factor. We therefore define off-resonance natural evolution, together with the Rabi frequencies and related interaction parameters in equation (35) or the original equation (10), in the general form

$$k = \nu\sqrt{\overline{n}}\ ; \quad \sqrt{\overline{n}} = \frac{1}{2}kf \quad \Rightarrow \quad f = \frac{2}{\nu}\ ; \quad \nu = 2\frac{\lambda}{\omega}$$

$$R_{n+j} = \lambda\sqrt{n+j+\left(\frac{\nu\sqrt{\overline{n}}-1}{\nu}\right)^2}\ ; \quad c_{n+j} = \frac{\left(\frac{\nu\sqrt{\overline{n}}-1}{\nu}\right)}{\sqrt{n+j+\left(\frac{\nu\sqrt{\overline{n}}-1}{\nu}\right)^2}}\ ; \quad s_{n+j} = \frac{\sqrt{n+j}}{\sqrt{n+j+\left(\frac{\nu\sqrt{\overline{n}}-1}{\nu}\right)^2}}$$

$$\overline{R}_{n+j} = \lambda\sqrt{n+j+\left(\frac{\nu\sqrt{\overline{n}}+1}{\nu}\right)^2}\ ; \quad \overline{c}_{n+j} = \frac{\left(\frac{\nu\sqrt{\overline{n}}+1}{\nu}\right)}{\sqrt{n+j+\left(\frac{\nu\sqrt{\overline{n}}+1}{\nu}\right)^2}}\ ; \quad \overline{s}_{n+j} = \frac{\sqrt{n+j}}{\sqrt{n+j+\left(\frac{\nu\sqrt{\overline{n}}+1}{\nu}\right)^2}} \tag{37}$$

This now constitutes the general synchronized form of off-resonance dynamics in the JC and aJC models. Since the numerical factor ν can be fixed within some specified ranges of values, $0 < \nu < 1$, $\nu = 1$, $1 < \nu < \infty$, the mean photon number amplitude $\sqrt{\overline{n}}$ becomes the only variable parameter in the natural evolution defined in equation (37). It follows easily from equation (37) that the evolution reduces to resonance $k = 1$ natural evolution at $\nu\sqrt{\overline{n}} = 1$, i.e., resonance is determined by $\nu = \overline{n}^{-\frac{1}{2}}$, noting a factor 4 arising in the reduced aJC model.

In characterizing the atomic state evolution over the entire mean photon number amplitude range $0 < \sqrt{\overline{n}} \leq 11.2$ for specified values of the numerical factor ν, we have established that,
(i) steady state time-independent evolution described by a maximally entangled state arises at $\sqrt{\overline{n}} \geq 11.2$, as in Fig.(9), completely independent of $\nu > 0$
(ii) within the range of small values $0 < \nu < 1$, setting $\nu \leq 0.01$ (i.e., $0 < \nu \leq 0.01$) generates steady state time-independent evolution described, respectively, by completely disentangled pure state in the regime $0 < \sqrt{\overline{n}} \leq 8.55$, precisely similar to the corresponding evolution within the same $\sqrt{\overline{n}}$ in Fig.14 example, mixed state in the regime $8.55 < \sqrt{\overline{n}} < 9.57$, precisely similar to the corresponding evolution in Fig.15 example and entangled state in the regime $9.57 \leq \sqrt{\overline{n}} < 11.2$, precisely similar to the corresponding evolution in

Fig.20 , Fig.21 examples; increasing ν into the range $0.01 < \nu < 1$ generates intermediate stage mixed states describing time-dependent periodic evolution
(iii) within the range of large values $\nu > 1$, setting $\nu \to \infty$ in equation (37) effectively reduces the off-resonance JC and aJC models to the resonance weak coupling aJC model defined by equation (29); for $\nu \to \infty$, off-resonance aJC dynamics is equivalent to the resonant aJC dynamics and effectively reproduces, all the dynamical features of natural evolution in resonant strong and weak coupling aJC dynamics within the corresponding ground state, mixed state and entangled state regimes plotted in the respective Fig.2 , Fig.4 , Fig.6 , Fig.8 , Fig.11-Fig.13 and Fig.16-Fig.19 examples; on the other hand, for $\nu \to \infty$, off-resonance JC dynamics reproduces only the ground state evolution in the small $\sqrt{\overline{n}}$ regime $0 < \sqrt{\overline{n}}$ of resonant JC dynamics plotted in Fig.1 example; we observe that $\nu = 20.755$ already gives the features $\nu \to \infty$; setting ν in the range $1 < \nu < 20.755$ also generates intermediate stage mixed states describing time-dependent periodic evolution

(iv) Optimal synchronized off-resonance evolution: $\nu = 1$
Setting $\nu = 1$ generates optimal synchronized off-resonance natural evolution controlled only by the mean photon number amplitude $\sqrt{\overline{n}}$ in the (entire) range $0 < \sqrt{\overline{n}} \leq 11.2$ in both JC and aJC models; setting $\nu = 1$ in equation (37) gives

$$\nu = 1$$

$$\text{JC}: \; R_{n+j} = \lambda\sqrt{n+j+(\sqrt{\overline{n}}-1)^2} \; ; \quad c_{n+j} = \frac{\sqrt{\overline{n}}-1}{\sqrt{n+j+(\sqrt{\overline{n}}-1)^2}} \; ; \quad s_{n+j} = \frac{\sqrt{n+j}}{\sqrt{n+j+(\sqrt{\overline{n}}-1)^2}}$$

$$\text{aJC}: \; \overline{R}_{n+j} = \lambda\sqrt{n+j+(\sqrt{\overline{n}}+1)^2} \; ; \quad \overline{c}_{n+j} = \frac{\sqrt{\overline{n}}+1}{\sqrt{n+j+(\sqrt{\overline{n}}+1)^2}} \; ; \quad \overline{s}_{n+j} = \frac{\sqrt{n+j}}{\sqrt{n+j+(\sqrt{\overline{n}}+1)^2}} \quad (38)$$

which reveals an important dynamical property that the synchronized off-resonance natural evolution at $\nu = 1$ generalizes resonance natural evolution at $f = \sqrt{\overline{n}}$ defined by equations (23) , (21′).

In general, for the entire range of values of the mean photon number amplitude $0 < \sqrt{\overline{n}} \leq 11.2$, the synchronized off-resonance natural evolution at $\nu = 1$ takes precisely similar forms in both JC and aJC models, except in the ground state evolution regime $0 < \sqrt{\overline{n}} \leq 0.02$, where the JC model does not generate excitations, causing only free evolution of the ground state exactly the same as in the resonance evolution in Fig.1, while the aJC model generates ground state excitations, causing transitions between the low-lying qubit states $|g0\rangle$ and $|e1\rangle$, with significantly different dynamical features compared to the resonance evolution in Fig.2.

For closer comparison, we have plotted the ground state evolution in off-resonance JC model in Fig.22 and in off-resonance aJC model in Fig.23, while in Fig.24, we compare the evolution of the ground state excitation number $\langle\sigma_-\sigma_+\rangle$ and the excited state excitation number $\langle\sigma_+\sigma_-\rangle$ in the aJC model.

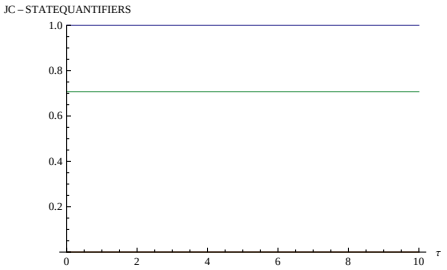

Figure 22: Off-resonance natural evolution of degree of atomic state purity $\overline{\mathcal{D}}$ (BLUE), concurrence $\overline{\mathcal{C}}$ (RED) and excitation number $\langle\sigma_+\sigma_-\rangle$ (YELLOW) in the JC model at $\nu = 1$; $\sqrt{\overline{n}} = 0.015$ (within the ground state evolution regime $0 < \sqrt{\overline{n}} \leq 0.02$) over scaled time $\tau = \lambda t$

The off-resonance evolution in Fig.22, exactly the same as the corresponding resonance evolution in Fig.1, demonstrates that the property that the JC model does not generate ground state excitations and transitions is an internal characteristic feature of the JC interaction mechanism, independent of the atom-field mode frequency detuning.

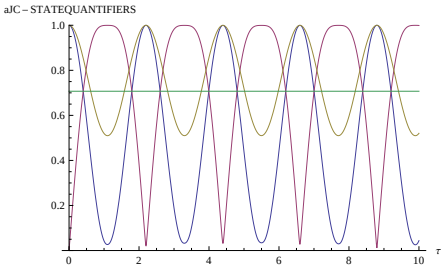

Figure 23: Off-resonance natural evolution of degree of atomic state purity $\overline{\mathcal{D}}$ (BLUE), concurrence $\overline{\mathcal{C}}$ (RED) and excitation number $\langle\sigma_-\sigma_+\rangle$ (YELLOW) in the aJC model at $\nu = 1$; $\sqrt{\overline{n}} = 0.015$ (within the ground state evolution regime $0 < \sqrt{\overline{n}} \leq 0.02$) over scaled time $\tau = \lambda t$

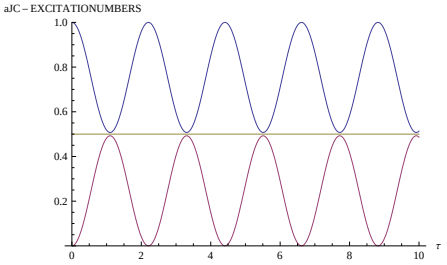

Figure 24: Off-resonance natural evolution of ground state excitation number $\langle\sigma_-\sigma_+\rangle$ (BLUE) and excited state excitation number $\langle\sigma_+\sigma_-\rangle$ (RED) in the aJC model at $\nu = 1$; $\sqrt{\overline{n}} = 0.015$ (within the ground state evolution regime $0 < \sqrt{\overline{n}} \leq 0.02$) over scaled time $\tau = \lambda t$; equal excitation number axis is (YELLOW)

The ground state evolution in the off-resonance aJC model in Fig.23 , Fig.24 reveals significantly different dynamical features compared to the corresponding resonance evolution in Fig.2: (i) the maximum of the concurrence (red) in Fig.23 is *much broader* compared to the corresponding sharp maximum in Fig.2, signifying that the periodically evolving entangled state in off-resonance aJC dynamics is *longer-lived* (ii) in Fig.23, the ground state spin excitation number $\langle\sigma_-\sigma_+\rangle$ (yellow) only undergoes periodic Rabi oscillations with maximum at 1 and minimum at $\frac{1}{2}$, while Fig.24 reveals the important property that the minimum value of the ground state spin excitation number (blue) coincides with the maximum value of the excited state spin excitation number $\langle\sigma_+\sigma_-\rangle$ (red) at $\langle\sigma_-\sigma_+\rangle = \langle\sigma_+\sigma_-\rangle = \frac{1}{2}$, signifying evolution in atomic coherent state or atom-field mode maximally entangled state, with equal probabilities, each $\frac{1}{2}$, to be in the ground or excited state; here, we note that the ground and excited state spin excitation numbers are equal to the probabilities to be in the ground and excited states, respectively.

Beyond the ground state evolution regime, synchronized off-resonance natural evolution in both JC and aJC models are similar, as in the examples at $\sqrt{\overline{n}} = 9.57$ in Fig.25 in the JC model and in Fig.26 in the aJC model. Notice that, as expected, the off-resonance evolution in Fig.25 , Fig.26 is essentially the same as the corresponding evolution at 9.57 in Fig.17 in resonant weak coupling aJC model.

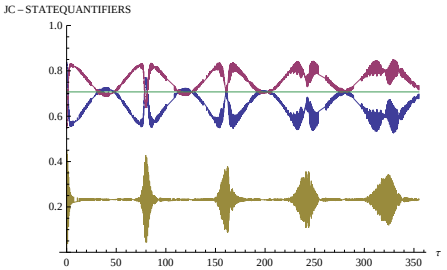

Figure 25: Off-resonance natural evolution of the degree of purity $\overline{\mathcal{D}}$ (BLUE), concurrence $\overline{\mathcal{C}}$ (RED) and spin excitation number $\langle\sigma_-\sigma_+\rangle$ (YELLOW) in the JC model at $\nu = 1$; $\sqrt{\overline{n}} = 9.57$ over scaled time $\tau = \lambda t$

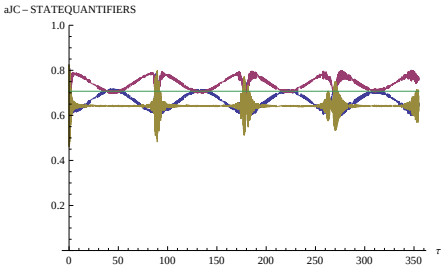

Figure 26: Off-resonance natural evolution of the degree of purity $\overline{\mathcal{D}}$ (BLUE), concurrence $\overline{\mathcal{C}}$ (RED) and spin excitation number $\langle \sigma_- \sigma_+ \rangle$ (YELLOW) in the aJC model at $\nu = 1$; $\sqrt{\overline{n}} = 9.57$ over scaled time $\tau = \lambda t$

Interestingly, the off-resonance JC, resonance aJC and off-resonance aJC natural evolution properties defined in equations (29) and (38) may be interpreted collectively as a triplet of optimal natural evolution at $(\sqrt{\overline{n}} - 1)$, $(\sqrt{\overline{n}})$, $(\sqrt{\overline{n}} + 1)$, well described by noting that the natural evolution profile of the concurrence (red) and degree of purity (blue) in off-resonance aJC model in Fig.17 lies in-between the corresponding profiles in off-resonance JC model in Fig.25 and aJC model in Fig.26.

We observe that, keeping $\sqrt{\overline{n}}$ at the natural evolution value in the various regimes over the entire range $0 < \sqrt{\overline{n}} \leq 11.2$, but decreasing ν to much smaller values $\nu \leq 0.01$, generates steady state time-independent evolution in completely disentangled pure state or stable mixed state or entangled state in the respective state evolution regimes. On the other hand, increasing ν to comparatively larger values $\nu > 0.01$ generates intermediate stage mixed states describing time-dependent periodic evolution.

Up to this stage, we have provided a fairly complete description of the main features of the characterization of the atomic state evolution, using the degree of purity, concurrence and spin excitation number in the JC and aJC models. In resonance natural evolution in section 3.2, we identified strong and weak coupling interactions specified by the residual detuning parameter values $0 < f < 1$ and $1 < f < \infty$ (i.e., $f < 1$; $f > 1$), respectively, thus leaving a gap at $f = 1$, which we identify as the intermediate coupling interaction regime. We now proceed to this case of intermediate coupling interaction, where we obtain an important composite physical state of the atom-field mode at resonance, specified by $k = 1$, $f = 1$, effectively defining *triple resonance* dynamics.

3.4 Resonant intermediate coupling interaction $(k = 1 \ ; \ f = 1)$: spin-displaced field modes

The subject of discussion in this section is an offshoot from sections 3.2 and 3.3, where we have presented interesting physical and fundamental quantum mechanical features of resonant $k = 1$ and off-resonant $k \neq 1$ atom-field interaction in the strong interaction regime characterized by the residual detuning parameter f values in the range $0 < f < 1$ and weak coupling interaction regime characterized by $1 < f < \infty$. It is evident in the above sections that we have not addressed the question on the nature of the dynamics at the intermediate coupling parameter value $f = 1$, which lies at the boundary of the strong coupling and weak coupling parameter values.

To complete the dynamical picture presented in sections 3.2 and 3.3, we develop the unique physical nature of the JC and aJC atom-field system in the resonant intermediate coupling interaction characterized by the detuning parameter values $k = 1$, $f = 1$. According to the parameter definitions $\omega_0 = k\omega$, $\omega = \lambda f$ in equation (8), the resonant intermediate coupling atom-field interaction in the JC and aJC models is governed by the frequency and coupling constant *triple resonance* relations

$$k = \frac{\omega_0}{\omega} \ ; \quad f = \frac{\omega}{g} \ ; \qquad k = 1 \ ; \quad f = 1 \quad \Rightarrow \quad g = \omega = \omega_0 \tag{38}$$

We are not aware of any work in the existing literature which focusses attention on the physical nature of the JC or aJC model under the triple resonance conditions given here in equation (38), particularly in the form we now proceed to develop briefly as JC and aJC spin-displaced field modes.

3.4.1 The JC spin-displaced field mode

Applying the triple resonance relation $g = \omega = \omega_0$ from equation (38) in equation (3) provides the JC qubit Hamiltonian $\mathcal{H}$ in the resonant intermediate coupling interaction in the form

$$g = \omega = \omega_0 \ : \qquad \mathcal{H}_{JC} = \hbar\omega(\hat{a}^\dagger\hat{a} + \sigma_+\sigma_- - \frac{1}{2} + \hat{a}\sigma_+ + \hat{a}^\dagger\sigma_-) = \hbar\omega(\hat{N} + \hat{\mathcal{R}}) \ ; \qquad \hat{\mathcal{R}} = \hat{a}\sigma_+ + \hat{a}^\dagger\sigma_- \quad (39)$$

where $\hat{N} = \hat{a}^\dagger\hat{a} + \sigma_+\sigma_- - \frac{1}{2}$ is the conserved JC excitation number operator defined in equation (3), while $\hat{\mathcal{R}}$ defined here in equation (39) is the qubit state transition operator in the resonant intermediate coupling interaction. We interpret the JC qubit Hamiltonian $\mathcal{H}_{JC}$ in equation (39) as the Hamiltonian of a quantized field mode of angular frequency ω driven by atomic spin, where the dynamics is characterized by the atom and field mode alternately emitting and absorbing photons in red-sideband transitions. Indeed, the Hamiltonian $\mathcal{H}_{JC}$ is factorizable in terms of spin-displaced field mode annihilation and creation operators $\hat{A}$, $\hat{A}^\dagger$ in the form

$$\hat{A} = \hat{a} + \sigma_- \ ; \quad \hat{A}^\dagger = \hat{a}^\dagger + \sigma_+ \ ; \qquad \mathcal{H}_{JC} = \hbar\omega\left(\hat{A}^\dagger\hat{A} - \frac{1}{2}\right) \quad (40)$$

In the form defined in equation (40), we specifically interpret $\mathcal{H}_{JC}$ as the Hamiltonian of a *JC spin-displaced field mode*, with state annihilation and creation operators $\hat{A}$, $\hat{A}^\dagger$, respectively.

To determine the eigenstate spectrum of the JC spin-displaced field mode, we consider an interaction starting from an atom-field initial state $|en\rangle$ with the atom in excited state $|e\rangle$ and field mode in number state $|n\rangle$. Applying the qubit state transition operator $\hat{\mathcal{R}}$ on the initial state $|en\rangle$, we obtain coupled qubit states ($|en\rangle$, $|gn+1\rangle$) and eigenstates $|\psi^\pm_{en}\rangle$ satisfying state transition and eigenvalue operations

$$\hat{\mathcal{R}}\ |en\rangle = \sqrt{n+1}\ |gn+1\rangle \ ; \qquad \hat{\mathcal{R}}\ |gn+1\rangle = \sqrt{n+1}\ |en\rangle \quad (41)$$

$$|\psi^\pm_{en}\rangle = \frac{1}{\sqrt{2}}\left(\ |en\rangle \pm |gn+1\rangle\ \right) : \qquad \hat{N}\ |\psi^\pm_{en}\rangle = \left(n + \frac{1}{2}\right)|\psi^\pm_{en}\rangle \ ; \qquad \hat{\mathcal{R}}\ |\psi^\pm_{en}\rangle = \pm\sqrt{n+1}\ |\psi^\pm_{en}\rangle$$

$$\mathcal{H}_{JC}\ |\psi^\pm_{en}\rangle = \mathcal{E}^\pm_{en}|\psi^\pm_{en}\rangle \ ; \qquad \mathcal{E}^\pm_{en} = \hbar\omega\left(n + \frac{1}{2} \pm \sqrt{n+1}\ \right) \quad (42)$$

The eigenstates $|\psi^\pm_{en}\rangle$ are orthonormal, satisfying the relations

$$\langle\psi^\pm_{en}|\psi^\pm_{en}\rangle = 1 \ ; \qquad \langle\psi^\pm_{en}|\psi^\mp_{en}\rangle = 0 \quad (43)$$

We have established that the qubit eigenstates $|\psi^\pm_{en}\rangle$ constitute the eigenstate spectrum of the JC spin-displaced field mode satisfying state transition and eigenvalue operations generated by the spin-displaced annihilation and creation operators $\hat{A}$, $\hat{A}^\dagger$ in the form

$$\hat{A}\ |\psi^\pm_{en}\rangle = |\phi^\pm_{en}\rangle \ ; \quad \hat{A}^\dagger\ |\phi^\pm_{en}\rangle = \left(n + 1 \pm \sqrt{n+1}\ \right)|\psi^\pm_{en}\rangle \ ; \quad |\phi^\pm_{en}\rangle = \frac{1}{\sqrt{2}}\left(\sqrt{n}\ |en-1\rangle + (1 \pm \sqrt{n+1}\ )|gn\rangle\right)$$

$$\mathcal{H}_{JC} = \hbar\omega\left(\hat{A}^\dagger\hat{A} - \frac{1}{2}\right) : \qquad \hat{A}^\dagger\hat{A}\ |\psi^\pm_{en}\rangle = \left(n + 1 \pm \sqrt{n+1}\ \right)|\psi^\pm_{en}\rangle \qquad \Rightarrow \qquad \mathcal{H}_{JC}\ |\psi^\pm_{en}\rangle = \mathcal{E}^\pm_{en}|\psi^\pm_{en}\rangle \quad (44)$$

We identify $\hat{A}^\dagger\hat{A}$ as the excitation number operator of the spin-displaced field mode, with number eigenvalues $n+1\pm\sqrt{n+1} = \sqrt{n+1}\left(\sqrt{n+1} \pm 1\right)$. As expected, the energy spectrum of the JC spin-displaced field mode agrees exactly with the energy spectrum of the equivalent JC qubit in equation (42). Finally, applying the eigenvalue equation (44), the spin-displaced field mode time evolution operator $\mathcal{U}_{JC}(t) = e^{-\frac{i}{\hbar}\mathcal{H}_{JC}t}$ generates time evolving eigenstates according to

$$\mathcal{U}_{JC}(t) = e^{-i\omega\left(\hat{A}^\dagger\hat{A} - \frac{1}{2}\right)t} : \qquad \mathcal{U}_{JC}(t)|\psi^\pm_{en}\rangle = e^{-i\mathcal{E}^\pm_{en}t}|\psi^\pm_{en}\rangle \quad (45)$$

Up to this stage, we have established that in the resonant intermediate coupling interaction state $g = \omega = \omega_0$, the JC qubit Hamiltonian $\mathcal{H}_{JC}$ in equation (39) constitutes a physically meaningful spin-displaced field mode with well defined spin-displaced annihilation and creation operators, Hamiltonian and eigenstate spectrum as presented in equations (40) , (42)-(45).

For completeness, we observe that the appropriate order operators for studying the dynamics of the JC spin-displaced field mode are the quadrature components $\hat{X}_1$, $\hat{X}_2$ defined by

$$\hat{X}_1 = \frac{1}{2}(\hat{A}^\dagger + \hat{A}) \; ; \qquad \hat{X}_2 = -\frac{i}{2}(\hat{A}^\dagger - \hat{A}) \tag{46}$$

In addition to the eigenvalue equations (44), we have obtained the following relations useful for determining the mean values, fluctuations and Heisenberg uncertainty product in measurements of the quadrature components in the eigenstates $|\psi_{en}^{\pm}\rangle$:

$$\langle\psi_{en}^{\pm}|\hat{A}|\psi_{en}^{\pm}\rangle = 0 \; ; \qquad \langle\psi_{en}^{\pm}|\hat{A}^\dagger|\psi_{en}^{\pm}\rangle = 0 \; ; \qquad \langle\psi_{en}^{\pm}|\hat{A}\hat{A}^\dagger|\psi_{en}^{\pm}\rangle = \left(n+1 \pm \sqrt{n+1}\,\right) + 1$$

$$\langle\psi_{en}^{\pm}|[\;\hat{A}\;,\;\hat{A}^\dagger\;]|\psi_{en}^{\pm}\rangle = 1 \tag{47}$$

The mean value of the commutator $[\;\hat{A}\;,\;\hat{A}^\dagger\;]$ obtained in equation (47) means that the JC spin-displaced field mode has bosonic properties in the eigenstate $|\psi_{en}^{\pm}\rangle$ computational space. Details of this beautiful JC spin-displaced field mode dynamics, with great potential for applications to quantum thermodynamics, will be presented elsewhere. We proceed to the corresponding aJC spin-displaced field mode.

3.4.2 The aJC spin-displaced field mode

In the resonant intermediate coupling interaction governed by the triple resonance relation $g = \omega = \omega_0$ in equation (40), the aJC qubit Hamiltonian $\mathcal{H}_{aJC}$ is obtained in the form

$$\mathcal{H}_{aJC} = \hbar\omega\left(\hat{a}\hat{a}^\dagger + \sigma_-\sigma_+ - \frac{1}{2} + \hat{a}\sigma_- + \hat{a}^\dagger\sigma_+\right) = \hbar\omega(\;\hat{\overline{N}} + \hat{\overline{\mathcal{R}}}\;) \; ; \qquad \hat{\overline{\mathcal{R}}} = \hat{a}\sigma_- + \hat{a}^\dagger\sigma_+ \tag{48}$$

where $\hat{\overline{N}} = \hat{a}\hat{a}^\dagger + \sigma_-\sigma_+ - \frac{1}{2}$ is the conserved aJC excitation number operator defined in equation (3), while $\hat{\overline{\mathcal{R}}}$ defined in equation (48) is the qubit state transition operator in the resonant intermediate coupling interaction. We interpret the aJC qubit Hamiltonian $\mathcal{H}_{aJC}$ in equation (48) as the Hamiltonian of a quantized field mode of angular frequency ω driven by atomic spin, where the dynamics is here characterized by simultaneous emission or absorption of photons by both atom and field mode in blue-sideband transitions.

The Hamiltonian $\mathcal{H}_{aJC}$ is factorizable in terms of spin-displaced field mode annihilation-creation operators $\hat{\overline{A}}$, $\hat{\overline{A}}^\dagger$ in the form

$$\hat{\overline{A}} = \hat{a} + \sigma_+ \; ; \quad \hat{\overline{A}}^\dagger = \hat{a}^\dagger + \sigma_- \; ; \qquad \mathcal{H}_{aJC} = \hbar\omega\left(\;\hat{\overline{A}}^\dagger\;\hat{\overline{A}} + \frac{1}{2}\right) \tag{49}$$

which provides the interpretation that $\mathcal{H}_{aJC}$ is the Hamiltonian of an aJC spin-displaced field mode with state annihilation-creation operators $\hat{\overline{A}}$, $\hat{\overline{A}}^\dagger$.

To determine the eigenstate spectrum of the aJC spin-displaced field mode, we consider an interaction starting from an atom-field initial state $|gn\rangle$ with the atom in ground state $|g\rangle$ and field mode in number state $|n\rangle$. Applying the qubit state transition operator $\hat{\overline{\mathcal{R}}}$ on the initial state $|gn\rangle$, we obtain coupled qubit states ($|gn\rangle$, $|en+1\rangle$) and eigenstates $|\;\overline{\psi}_{gn}^{\pm}\rangle$ satisfying state transition and eigenvalue operations

$$\hat{\overline{\mathcal{R}}}\;|gn\rangle = \sqrt{n+1}\;|en+1\rangle \; ; \qquad \hat{\overline{\mathcal{R}}}\;|en+1\rangle = \sqrt{n+1}\;|gn\rangle \tag{50}$$

$$|\;\overline{\psi}_{gn}^{\pm}\rangle = \frac{1}{\sqrt{2}}\,(\;|gn\rangle \pm |en+1\rangle\;) : \qquad \hat{\overline{N}}\;|\;\overline{\psi}_{gn}^{\pm}\rangle = \left(n+\frac{3}{2}\right)|\;\overline{\psi}_{gn}^{\pm}\rangle \; ; \qquad \hat{\overline{\mathcal{R}}}\;|\psi_{gn}^{\pm}\rangle = \pm\sqrt{n+1}\;|\;\overline{\psi}_{gn}^{\pm}\rangle$$

$$\mathcal{H}_{aJC}\;|\;\overline{\psi}_{gn}^{\pm}\rangle = \overline{\mathcal{E}}_{gn}^{\pm}|\;\overline{\psi}_{gn}^{\pm}\rangle \; ; \qquad \overline{\mathcal{E}}_{gn}^{\pm} = \hbar\omega\left(n+\frac{3}{2} \pm \sqrt{n+1}\;\right) \tag{51}$$

The eigenstates $|\;\overline{\psi}_{gn}^{\pm}\rangle$ are orthonormal, satisfying the relations

$$\langle\;\overline{\psi}_{gn}^{\pm}|\;\overline{\psi}_{gn}^{\pm}\rangle = 1 \; ; \qquad \langle\;\overline{\psi}_{gn}^{\pm}|\;\overline{\psi}_{gn}^{\mp}\rangle = 0 \tag{52}$$

We have established that the qubit eigenstates $|\,\overline{\psi}^{\pm}_{gn}\rangle$ constitute the eigenstate spectrum of the aJC spin-displaced field mode satisfying state transition and eigenvalue operations generated by the spin-displaced annihilation-creation operators $\hat{\overline{A}}$, $\hat{\overline{A}}^{\dagger}$ in the form

$$\hat{\overline{A}}\,|\,\overline{\psi}^{\pm}_{gn}\rangle = |\,\overline{\phi}^{\pm}_{gn}\rangle\,; \quad \hat{\overline{A}}^{\dagger}\,|\,\overline{\phi}^{\pm}_{gn}\rangle = \big(n+1\pm\sqrt{n+1}\,\big)\,|\,\overline{\psi}^{\pm}_{gn}\rangle\,; \quad |\,\overline{\phi}^{\pm}_{gn}\rangle = \frac{1}{\sqrt{2}}\left(\sqrt{n}\;|gn-1\rangle + (1\pm\sqrt{n+1}\,)|en\rangle\right)$$

$$\mathcal{H}_{aJC} = \hbar\omega(\,\hat{\overline{A}}^{\dagger}\hat{\overline{A}} + \frac{1}{2}) : \qquad \hat{\overline{A}}^{\dagger}\hat{\overline{A}}\,|\,\overline{\psi}^{\pm}_{gn}\rangle = \big(n+1\pm\sqrt{n+1}\,\big)\,|\,\overline{\psi}^{\pm}_{gn}\rangle \qquad \Rightarrow \qquad \mathcal{H}_{aJC}\,|\,\overline{\psi}^{\pm}_{gn}\rangle = \overline{\mathcal{E}}^{\pm}_{gn}|\,\overline{\psi}^{\pm}_{gn}\rangle \tag{53}$$

We identify $\hat{\overline{A}}^{\dagger}\hat{\overline{A}}$ as the excitation number operator of the spin-displaced field mode, with number eigenvalues $n+1\pm\sqrt{n+1} = \sqrt{n+1}\left(\sqrt{n+1}\pm 1\right)$. As expected, the energy spectrum of the aJC spin-displaced field mode agrees exactly with the energy spectrum of the equivalent aJC qubit in equation (51).

Applying the eigenvalue equation (53), the spin-displaced field mode time evolution operator $\mathcal{U}_{aJC}(t) = e^{-\frac{i}{\hbar}\mathcal{H}_{aJC}t}$ generates time evolving eigenstates according to

$$\mathcal{U}_{aJC}(t) = e^{-i\omega\left(\,\hat{\overline{A}}^{\dagger}\hat{\overline{A}}+\frac{1}{2}\right)t} : \qquad \mathcal{U}_{aJC}(t)|\,\overline{\psi}^{\pm}_{gn}\rangle = e^{-i\overline{\mathcal{E}}^{\pm}_{gn}t}|\,\overline{\psi}^{\pm}_{gn}\rangle \tag{54}$$

We have thus established that in the resonant intermediate coupling interaction state $g=\omega=\omega_0$, the aJC qubit Hamiltonian $\mathcal{H}_{aJC}$ in equation (48) constitutes a spin-displaced field mode with well defined spin-displaced annihilation-creation operators, Hamiltonian and eigenstate spectrum as presented in equations (49) , (51)-(54).

The appropriate order operators for studying the dynamics of the aJC spin-displaced field mode are the quadrature components $\hat{\overline{X}}_1$, $\hat{\overline{X}}_2$ defined by

$$\hat{\overline{X}}_1 = \frac{1}{2}(\,\hat{\overline{A}}^{\dagger} + \hat{\overline{A}}\,)\,; \qquad \hat{\overline{X}}_2 = -\frac{i}{2}(\,\hat{\overline{A}}^{\dagger} - \hat{\overline{A}}\,) \tag{55}$$

We have obtained the following relations useful for determining the mean values, fluctuations and Heisenberg uncertainty product in measurements of the quadrature components in the eigenstates $|\,\overline{\psi}^{\pm}_{gn}\rangle$:

$$\langle\,\overline{\psi}^{\pm}_{gn}|\,\hat{\overline{A}}|\,\overline{\psi}^{\pm}_{gn}\rangle = 0\,; \qquad \langle\,\overline{\psi}^{\pm}_{gn}|\,\hat{\overline{A}}^{\dagger}\,|\,\overline{\psi}^{\pm}_{gn}\rangle = 0\,; \qquad \langle\,\overline{\psi}^{\pm}_{gn}|\,\hat{\overline{A}}\,\hat{\overline{A}}^{\dagger}\,|\,\overline{\psi}^{\pm}_{gn}\rangle = \big(n+1\pm\sqrt{n+1}\,\big)+1$$

$$\langle\,\overline{\psi}^{\pm}_{gn}|[\,\hat{\overline{A}}\,,\,\hat{\overline{A}}^{\dagger}\,]|\,\overline{\psi}^{\pm}_{en}\rangle = 1 \tag{56}$$

The mean value of the commutator $[\,\hat{\overline{A}}\,,\,\hat{\overline{A}}^{\dagger}\,]$ obtained in equation (56) means that the aJC spin-displaced field mode has bosonic properties in the eigenstate $|\,\overline{\psi}^{\pm}_{gn}\rangle$ computational space. Details of the aJC spin-displaced field mode dynamics, with great potential for applications to quantum thermodynamics, will be presented elsewhere.

We close this brief presentation of the JC and aJC spin-displaced field modes by giving an interesting physical interpretation. Comparing the eigenvalue equations (44) and (53) reveals that the JC and aJC spin-displaced mode number operators $\hat{A}^{\dagger}\hat{A}$, $\hat{\overline{A}}^{\dagger}\,\hat{\overline{A}}$, respectively, have the same eigenvalue (same excitation number) $n+1\pm\sqrt{n+1}$. This is attributed to the property that the JC and aJC number operators and the corresponding Hamiltonians $\mathcal{H}_{JC}$, $\mathcal{H}_{aJC}$ are duality symmetry conjugates, related by a duality symmetry transformation well developed in [3]. The duality symmetry operation transforms the atomic spin states according to $|g\rangle \rightarrow |e\rangle$, $|e\rangle \rightarrow |g\rangle$, with an associated global phase factor in each case. In this respect, the JC and aJC spin-displaced mode eigenstates $|\psi^{\pm}_{en}\rangle$, $|\psi^{\pm}_{gn}\rangle$ defined in equations (42) , (51) are orthogonal duality symmetry conjugates, noting that the transformation generates an associated global phase factor. If we now include a transformation property $\omega \rightarrow -\omega$ (not considered in [3]), then the full operation of the duality symmetry transformation leads to the interesting physical interpretation that the JC and aJC spin-displaced modes are duality symmetry conjugates, with respective energy spectra $\mathcal{E}^{\pm}_{en}$, $\overline{\mathcal{E}}^{\pm}_{gn}$ in equations (42) , (51), noting that the transformation $\omega \rightarrow -\omega$ may give $\overline{\mathcal{E}}^{\pm}_{gn}$ an overall negative sign. Details of the potentially exciting duality symmetry conjugation property of the JC and aJC spin-displaced field modes will be developed elsewhere in a general context of the full quantum Rabi model in which the spin-displaced field mode Hamiltonians in equations (39) , (48) arise in a general context at critical coupling constant $\lambda_c = 2g_c = \sqrt{\omega\omega_0}$ where the quantum Rabi model and the JC model undergo a quantum phase transition [16 , 17].

4 Conclusion

In the characterization of the atomic state evolution in the Jaynes-Cummings (JC) and anti-Jaynes-Cummings (aJC) models, we have established the following important dynamical properties of the atom-field mode interaction in the quantum Rabi model: (i) the aJC model has a non-vanishing residual detuning parameter $f > 0$, meaning that the aJC and therefore, the full quantum Rabi, interaction mechanism is intrinsically detuned, whereas the JC detuning parameter vanishes at resonance (ii) in the aJC model, the atomic initial ground state $|g0\rangle$ is occupied, having excitation number $\langle g0|\ \hat{\overline{N}}|g0\rangle = \frac{3}{2}$, and the aJC interaction mechanism generates blue-sideband qubit transitions from an initial ground state $|g0\rangle$, characterized by pure Rabi oscillations between the qubit states $|g0\rangle$ and $|e1\rangle$ in the small mean photon number range $0 < \sqrt{\overline{n}} \leq 0.1$; the ground state $|g0\rangle$ is an eigenstate of the JC Hamiltonian, which therefore cannot generate transitions from an initial ground state (iii) since resonant JC interaction is completely independent of the residual detuning parameter $f > 0$, the atomic state evolution over scaled time $\tau = \lambda t$ in resonant JC model is independent of coupling strength defined by f, thus taking the same form in the strong $0 < f < 1$ and weak $f > 1$ coupling interaction, and only spontaneously develops into a short-lived nearly pure state in the middle of the first collapse period of the spin excitation number (or atomic state population inversion) within the mean photon number amplitude range $1 < \sqrt{\overline{n}} \leq 8.55$; this spontaneous evolution to a nearly pure state is not a steady state property, but may be an internal natural coherence property of the atom; for larger mean photon number amplitude $\sqrt{\overline{n}} > 8.55$, the atomic state evolution develops into mixed and entangled state evolution regimes, then into a maximally entangled state at $\sqrt{\overline{n}} \geq 11.2$, meaning that the usual efforts towards disentangling the short-lived pure state in the very large mean photon number $\overline{n} \to \infty$ limit may be far-fetched approximations (iv) unification of the mean photon number amplitude $\sqrt{\overline{n}}$ and the detuning parameters f , k generates natural evolution property signifying atom in a uniformly mixed state in the aJC model and in the off-resonance (detuned) JC model, each composed of well defined ground state, mixed state and entangled state evolution regimes; in the resonant strong coupling $0 < f < 1$ aJC model, the atomic state evolution is characterized by pure Rabi oscillations within the ground state regime, developing collapses and revivals in the mixed state evolution regime where the atomic state spontaneously evolves to a short-lived nearly pure state precisely similar to the corresponding evolution in the resonant JC model described above ; increasing the residual detuning parameter f to very large values $f \to \infty$ in the resonance $k = 1$ aJC model, and similarly, decreasing the detuning parameter k to comparatively very small values $k \leq 0.01\sqrt{\overline{n}}$ in off-resonance $k \neq 1$ JC and aJC models, generates steady state time-independent evolution of the degree of purity, concurrence and spin excitation number at their appropriate maximum or minimum values, signifying the atom in an exact completely disentangled pure state, stable mixed state or stable entangled state describing steady state dynamics at very large residual detuning $f \to \infty$ in resonance aJC model or comparatively very small detuning $k \leq 0.01\sqrt{\overline{n}}$ in off-resonance JC and aJC models (v) at triple resonance $\lambda = \omega = \omega_0$, which occurs at $k = 1$, $f = 1$, the atom-field mode interaction in the quantum Rabi model reduces to duality symmetry conjugate JC and aJC spin-displaced field modes with well defined spectrum of energy eigenstates and eigenvalues.

5 Acknowledgement

I thank Maseno University for providing facilities and a conducive work environment during the preparation of the manuscript.

References

[1] J Akeyo Omolo 2017, Conserved excitation number and U(1)-symmetry operators for the antirotating (anti-Jaynes-Cummings) term of the quantum Rabi Hamiltonian, ResearchGate: DOI:10.13140/RG.2.2.30936.80647 ; arXiv:2103.06577 [quant-ph]

[2] J Akeyo Omolo 2021, The anti-Jaynes-Cummings model is solvable : quantum Rabi model in rotating and counter-rotating frames; following the experiments, arXiv:2103.09546 [quant-ph] ; htpp:/doi.org/10.21203/rs.3.rs-379917/v1

[3] J Akeyo Omolo 2021, Duality symmetry conjugates of the quantum Rabi model : effective bosonic, fermionic and coupling-only dynamical properties, arXiv:2112.12514 [quant-ph]

[4] E T Jaynes, F W Cummings 1963 Comparison of quantum and semiclassical radiation theories with application to the beam maser, Proc.IEEE **51**, 89

[5] J Koch, G R Hunanyan, T Ockenfels, E Rico, E Solano, M Weitz 2023 Quantum Rabi dynamics of trapped atoms far in the deep strong coupling regime, Nat.Commun.**14**, 954

[6] J Gea-Banacloche 1990 Collapse and revival of the state vector in the Jaynes-Cummings model : an example of state preparation by a quantum apparatus, Phys.Rev.Lett.**65**, 3385

[7] J Gea-Banacloche 1991, Phys.Rev.**A44**, 5913

[8] J Gea-Banacloche 1992 A new look at the Jaynes-Cummings model for large fields : Bloch sphere evolution and detuning effects, Opt. Commun.**88**, 531

[9] S J D Phoenix, P L Knight 1991, Establishment of an entangled atom-field state in the Jaynes-Cummings model, Phys.Rev.**A44**, 6023

[10] V Buzek , H Moya-Cessa , P L Knight , S J D Phoenix 1992, Schroedinger-cat states in the resonant Jaynes-Cummings model : collapse and revival of oscillations of the photon-number distribution, Phys.Rev.**A45**, 8190

[11] A Z Goldberg , A M Steinberg, 2020, Transcoherent states : optical states for maximal generation of atomic coherence, PRX **QUANTUM 1**, 020306

[12] H Dai , S Fu , S Luo 2020, Atomic nonclassicality in the Jaynes-Cummings model, Phys. Lett.**A384**, 126371

[13] J Akeyo Omolo 2022, On atomic state purity operator, degree of purity and concurrence in the Jaynes-Cummings and anti-Jaynes-Cummings models, arXiv:2207.02730 [quant-ph]

[14] J Akeyo Omolo 2018, Polariton and antipolariton qubits in the quantum Rabi model, ResearchGate: DOI:10.13140/RG.2.2.11833.67683

[15] C Mayero 2023, Photon statistics and quantum field entropy in the anti-Jaynes-Cummings model: a comparison with the Jaynes-Cummings interaction, Quantum Inf Process **22**, 182

[16] M J Hwang, R Puebla, M B Plenio 2015, Quantum phase transition and universal dynamics in the Rabi model, Phys.Rev.Lett. **115**, 180404 ; arXiv:1503.03090 [quant-ph]

[17] M J Hwang, M B Plenio 2016, Quantum phase transition in the finite Jaynes-Cummings lattices, arXiv:1603.03943 [quant-ph]